General Disclaimer

One or more of the Following Statements may affect this Document

- This document has been reproduced from the best copy furnished by the organizational source. It is being released in the interest of making available as much information as possible.

- This document may contain data, which exceeds the sheet parameters. It was furnished in this condition by the organizational source and is the best copy available.

- This document may contain tone-on-tone or color graphs, charts and/or pictures, which have been reproduced in black and white.

- This document is paginated as submitted by the original source.

- Portions of this document are not fully legible due to the historical nature of some of the material. However, it is the best reproduction available from the original submission.

E83-10365

CSC/TM-81/6238

CR-172893

APPLICATION OF SEASAT-1 SYNTHETIC APERTURE RADAR (SAR) DATA TO ENHANCE AND DETECT GEOLOGICAL LINEAMENTS AND TO ASSIST LANDSAT LANDCOVER CLASSIFICATION MAPPING

Prepared For

NATIONAL AERONAUTICS AND SPACE ADMINISTRATION
Goddard Space Flight Center
Greenbelt, Maryland

CONTRACT NAS 5-24350
Task Assignment 02402

SEPTEMBER 1981

(E83-10365) APPLICATION OF SEASAT-1 SYNTHETIC APERTURE RADAR (SAR) DATA TO ENHANCE AND DETECT GEOLOGICAL LINEAMENTS AND TO ASSIST LANDSAT LANDCOVER CLASSIFICATION MAPPING (Computer Sciences Corp.) 124 p

N83-29776

G3/43

Unclas
00365

CSC

COMPUTER SCIENCES CORPORATION

CSC/TM-81-6238

APPLICATION OF SEASAT-1 SYNTHETIC APERTURE RADAR (SAR) DATA TO ENHANCE AND DETECT GEOLOGICAL LINEAMENTS AND TO ASSIST LANDSAT LANDCOVER CLASSIFICATION MAPPING

Prepared for

GODDARD SPACE FLIGHT CENTER

By

COMPUTER SCIENCES CORPORATION

Under

Contract NAS 5-24350
Task Assignment 02402

Prepared by:

R. S. Sekhon 9/25/81
R. Sekhon Date

Approved by:

Ranjit Dasgupta 9/29/81
R. Dasgupta Date
Section Manager

Fred J. Gunther 9/25/81
Dr. F. J. Gunther Date
Quality Assurance
Reviewer

K C Lee 10/9/81
Dr. P. V. Rigterink Date
Technical Area Manager

ACKNOWLEDGMENTS

The author wishes to thank the many people who have contributed to this document.

Dr. Herbert Blodget, of Eastern Regional Remote Sensing Applications Center, Goddard Space Flight Center, encouraged and provided support for the activities described in this report. The development of the report involved contributions from Mr. James Roueche of Kentucky-Ohio-West Virginia Interstate Planning Commission, Dr. Dewey Sanderson, Dr. Richard Bonnett and professor James Brumfield of Marshall University, Dr. Peter Lessing of the West Virginia Geologic and Economic Survey, and Dr. William Adams of Eastern Kentucky University. Their contributions are shown in Appendixes A, B, C, D, and E, which were incorporated into the subsection on Lineament Evaluation and Classification Evaluation. Special thanks are due to Dr. Fred Gunther, of Computer Sciences Corporation, for his contributions in editing the document. Thanks to Ranjit Dasgupta and Dr. Paul Rigterink for providing encouragement, guidance and managerial support throughout the study. Thanks also to Karen Lindstrom, John Martin and other members of the Technical Publications staff who patiently and quickly responded to review changes in the text.

ABSTRACT

Digital Seasat-1 Synthetic Aperture Radar (SAR) data can be used to enhance linear features to extract geologically significant lineaments. This has been accomplished in the Appalachian region. Lineaments thus mapped were compared with an existing lineament map based on Landsat multispectral scanner (MSS) images. Results of this study showed that appropriately processed Seasat-1 SAR data can significantly improve the detection of lineaments. Lineament maps derived from Seasat SAR images will greatly enhance the information base for local and regional geological planning and resource utilization.

The best enhancements of both Seasat SAR and Landsat MSS images for lineament plotting were obtained using a simple contrast stretch. This procedure expands the original range of digital values to the full range of the image display device. A number of other contrast-enhancement methods were tested and judged inferior to this method.

A merge of Landsat-MSS/Seasat-SAR data increased the information content of the data sets. The information from one system was complementary to the other.

The merged data sets were found to be more useful for lineament detection and landcover classification than the Landsat or Seasat data alone. An analysis of a Seasat SAR image for lineaments detected more lineaments than found in the Landsat image for the same region. There was about 80 percent coincidence between lineaments plotted from Landsat and Seasat, whereas only 13 percent coincidence is reported in literature between lineaments from different sources. The estimate based on straight lineaments indicate that about 20 percent of the lineaments plotted from the Seasat SAR image did not appear on the Landsat image. About 6 percent

of minor lineaments or parts of lineaments present in the Landsat lineament map were missing from the Seasat lineament map.

An improvement in the landcover classification in acreage and spatial estimation accuracy was attained by using the Landsat-MSS/Seasat-SAR merged data instead of using Landsat MSS data. In particular, an improvement in the areal estimation of residential/built-up and forest categories was noticed. A slight reduction in accuracy in the estimation of the agricultural and water categories was found.

TABLE OF CONTENTS

TABLE OF CONTENTS (Cont'd)

LIST OF ILLUSTRATIONS

Figure

LIST OF TABLES

Table

LIST OF TABLES (Cont'd)

SECTION 1 - INTRODUCTION

Geologically significant photo-linear features, better-known as lineaments, are closely related to geological fracturing. The delineation of these features is important for natural-resource evaluation and exploration. Landsat Multispectral Scanner (MSS) and Seasat-1 Synthetic Aperture Radar (SAR) image data in particular afford geologists a synoptic view of a region. The synoptic view aids in the detection of regional linear features.

This report describes the technical phase of an Eastern Regional Remote Sensing Applications Center (ERRSAC) project conducted in cooperation with the Appalachian Regional Commission (ARC). The project was designed to evaluate image enhancement techniques used with both Landsat and Seasat imagery to detect lineaments for a part of the Appalachian region. This region is underlain by Devonian shale and is a known producer of oil and gas. Lineaments mapped on images can be related to geological structures, which in turn can be related to oil and gas deposits. The project will aid in the search for new fields and the expansion of others already drilled.

One purpose of this study was to determine if a simple, low-cost method exists for enhancing and detecting lineaments. The method had to be usable in an area of rapidly changing relief with heavy vegetation cover.

This report has been divided into seven sections. Section 2 discusses the nature and importance of lineaments, particularly for the benefit of non-geologists, who may be interested in the Landsat/Seasat data merge technique for other applications. It also gives a brief history of the previous work performed for enhancement of lineaments. Section 3 discusses the ARC study area for this project. The study

area included Cabell County and parts of surrounding counties in West Virginia. Section 4 describes the data characteristics, data acquisition procedures and image processing systems. Visual enhancement techniques for lineaments are described in Section 5. The Landsat/Seasat data-merger procedure and plotting of Seasat lineaments are described in detail. The landcover classification based on Landsat data and on Landsat/Seasat merged data is described and evaluated in Section 6. Concluding remarks are presented in Section 7.

Enhanced imagery of Landsat MSS, Seasat-1 SAR and Landsat-MSS/Seasat-SAR merged data were sent to participating geologists and planners for their evaluation on the applicability of the Seasat and the Landsat-MSS/Seasat-SAR merged imagery for lineament detection and mapping. The communications received from them are given in Appendixes A and B. Their findings were incorporated in Section 5.5.

Classified images for Landsat and Landsat/Seasat merged data were sent to participating geologists and planners in West Virginia and Kentucky for verification and evaluation. The private communications received from them are given in Appendixes C, D, and E. Their evaluations are included in Section 6.2.

SECTION 2 - BACKGROUND

2.1 REMOTE SENSING

The term "remote sensing" refers to data acquisition by sensors which are not in direct contact with the phenomena under observation (Reference 41). Sensors can be placed on an aircraft, a high altitude balloon, or a space satellite. The sensors can detect electromagnetic radiation such as visible light, infrared radiation, and similar forms of wave-transmitted energy. An active system both transmits the electromagnetic signal and receives the backscattered/reflected signal. Synthetic Aperture Radar (SAR) on the satellite Seasat-1 is an active microwave sensor. A passive system is a receiver only, requiring a natural source of energy, such as solar radiation. The multispectral scanner (MSS) on Landsat 1, originally known as Earth Resources Technology Satellite (ERTS-1), and on Landsats 2 and 3, is a passive system.

2.1.1 GENERAL USE

Remotely sensed data has many applications in geology, agriculture, forestry, urban planning, and various other research and planning activities (Reference 41). Landsat MSS data is now being applied to a wide variety of specific geologic problems that are difficult to solve by conventional methods alone, including mineral and energy resource exploration, nuclear power plant siting and waste disposal, and the charting of glaciers and shallow seas (Reference 1). In geology, aerial photography and remotely sensed imagery are utilized primarily to prepare geologic maps that depict stratigraphic units and surface-expressed structures. The structures may be favorable to localization of oil and gas at depth (Reference 42). These maps form the data base for deciding where to conduct geophysical surveys and eventual

exploratory drillings. Lineament mapping has become an important aspect of geologic mapping for mineral and oil exploration.

2.1.2 MULTISPECTRAL SCANNER (MSS)

Landsat 1 was launched on July 23, 1972 followed by Landsat 2 on January 22, 1975 and Landsat 3 on March 5, 1978. Each satellite carries two imaging systems, a Return Beam Vidicon (RBV) and a Multispectral Scanner (MSS).

The data are collected at an altitude of 918 km in a sun-synchronous orbit. The orbit of each working satellite is maintained so that it may image any location on the Earth every 18 days. The output from both RBV and MSS systems is converted into digital format for further processing. After processing, the data is available in the form of finished photoproducts or in the form of computer compatible tapes (CCTs), which can be further analyzed and refined using digital analysis techniques. Data in both forms can be purchased from the Earth Resources Observation Satellite (EROS) Data Center, Sioux Falls, S.D.

The discussion in this paper refers only to the MSS data. The MSS is a line-scanning device with swath 185 km wide in four spectral channels, which are numbered 4, 5, 6, and 7. The Landsat MSS channels, the spectral region, and landcover applications are shown in Table 2-1 (Reference 43).

One principal use of this multispectral capability stems from a basic property of materials. Various types of matter reflect differing amounts of light at different wavelengths or wavelength intervals. Because of this, they can be separated and identified by their own characteristic reflectance patterns, or spectral "signatures." This allows maps of landcover types to be prepared from MSS data.

Table 2-1. Landsat MSS Channels, Spectral Region and Landcover Applications (Taken From Reference 43)

Landsat MSS Channel	Spectral Region (μm)	Land Cover Application
Band 4	0.5-0.6 (Green)	Discriminates qualitatively the depth and/or turbidity of standing bodies of water
Band 5	0.6-0.7 (Red)	Best for showing topographic and cultural features, such as roads, cities
Band 6	0.7-0.8 (Near infrared)	Best for showing tonal contrasts that reflect various land use practices
Band 7	0.8-1.1 (Near infrared)	Best for land-water discrimination

2.1.3 SYNTHETIC APERTURE RADAR (SAR)

The Seasat-1 ocean-surveying satellite was launched on June 29, 1978 and was operational until October 10, 1978. During its short life span it obtained extensive coverage of land in the continental United States.

The Synthetic Aperture Radar (SAR) was one of five sensors onboard. This SAR is an L-band like-polarized (HH) radar operated at 1.27 GHz (23.5 cm) with excellent cloud and rain penetration capability (Reference 28). The antenna illuminated a swatn of 100 km, and provided spatial resolution of 25 meters in both range and azimuth directions. SAR images represent the reflectivity of the surface in the backscatter direction at the operating frequency. The image brightness is directly proportional to the surface backscatter cross-section. The data are generally obtained from the upper micrometers or millimeters of the surface because of the high opacity and scattering characteristics of natural materials (Reference 13).

In the decimeter spectral region, the backscatter energy is dependent primarily on surface physical properties such as average slope, small-scale roughness, and the surface and near-surface dielectric constant (a function of the surface composition, cover and moisture content). The tone and texture in the radar image provide new information that is not available with optical and infrared sensors. With Seasat SAR, the image may not be used for quantitative measurements because the system was not calibrated, and a number of non-linear processes such as clipping and saturation are inherent in some of the preliminary products.

Seasat SAR data can be obtained from the Environmental Data and Information Service, Satellite Data Services Division, Room 606, World Weather Building, Washington, D.C. Additional information on Synthetic Aperture Radar and data banks of existing SAR imagery may be found in NASA reference publication 1039 (Reference 28).

2.2 LINEAMENTS

2.2.1 GENERAL DISCUSSION

Lineaments are generally defined as "the significant lines of a landscape which reveal the hidden architecture of rock formation" (Reference 17). Examples of lineaments are the alignment of straight segments of valleys or alternating linear zones of varying brightness in an image. Lineaments frequently represent zones of weakness in the Earth's crust which may be due either to geological faults or joints controlled at least in part by faults; structural displacement is not a requirement for defining a lineament. Some operational definitions are very useful in visually interpreting and mapping lineaments from Landsat and Seasat imagery. Lineaments are:

- Dark lines of variable length, straightness, and continuity, that contrast with the lighter-toned background
- Sharp linear truncations of patterns and colored areas
- Alignments of drainage patterns, especially short stream segments
- Alignments of topographic forms, usually emphasized by shadowing
- Alignments of cultural features, where controlled by topography or by geologic structures

Wilson (Reference 53) recognized that large structural features can be better seen in aerial photographs than on the ground. The view of the surface of the Earth from space often enhances linear features that "... would be less apparent on conventional aerial photographs because of the limited aerial coverage of single prints and the abundance of distracting detail resolved at larger scale" (Reference 15). Structural features are not easily confused with anything else, but it is not alwasy easy to determine what type of structure is there. The information provided by satellite remote sensing can be used to focus more costly surface geophysical techniques, such as surface mapping or seismic, gravity, and electrical resistivity measurements, on a structural feature with potential economic or scientific value (Reference 43).

Lineaments can best be seen on digitally enhanced remotely sensed images (Sections 2.2.2.3 and 5.3). There are a number of digital image processing algorithms for the enhancement of remotely sensed images. Enhanced imagery can then be used to locate lineaments. Landsat and Seasat images are useful for mapping both the regional and local lineaments.

Lineaments interpreted from remotely sensed images should be evaluated in terms of geologic structures with caution. Werner (Reference 48) cautioned that such lineaments should be used as an aid in interpretation and not a controlling influence in arriving at any conclusion. He further reported that the relationship between observed lineaments and actual rock fractures was poorly known and the maximum coincidence between any two photo-lineaments was about 13 percent.

The author of this report agrees that caution is needed (see Section 5 for a discussion of consistency in mapping linears) but considers Werner to be over cautious.

Application of Seasat-1 SAR imagery for interpretation of lineaments has been reported in the literature only recently (Reference 10), perhaps due to the previous lack of availability of recent flight data. Synthetic Aperture Radar/Landsat image registration was discussed in detail by Maurer, et al. (References 28 and 29). They enumerated the difficulties encountered in merging (registering) the two data sets. Definition of the major applications and requirements for overlaying microwave and MSS data sets was investigated by Chafaris (Reference 6) in consultation with scientists in the various remote sensing disciplines.

2.2.2 PREVIOUS WORK

Numerous papers have been published detailing the geologic utility of lineament studies using remotely sensed data. Only a sample of such papers are summarized here.

2.2.2.1 Pre-Landsat Photointerpretation

Prior to the launch of the Landsat satellites, there were several studies of linear features detected in space photography. Mercury and earlier unmanned flights indicated the potential value of orbital and suborbital photographs for geologic and geographic analysis (Reference 26). Gemini flights included Synoptic Terrain Photographic Experiments using hand-held 70mm cameras, and later multispectral camera arrays. Such photography provided synoptic views of both known and previously undetected lineaments, correlated in some cases with known faults (References 15, 26, and 27). Such studies first indicated and then proved that linear features could be more easily detected using color infrared photography and lower sun angles (References 15 and 26).

2.2.2.2 Landsat Photointerpretation

Detection and analysis of Landsat lineaments using conventional photointerpretation and map comparisons have been

successful in detecting geologic patterns related to fractures and faults (Reference 40, page 7). Conventional photointerpretation is common because of the availability of Landsat images in photographic form (Reference 5). Houston, et. al. considered that visual inspection of Landsat images suggested the existence of extensions of known fault systems; they also reported a strong similarity in lineament orientation between the Laramie Basin and the Laramie Range (Reference 19). Isachsen (Reference 20) and Isachsen, et al., (Reference 21) found numerous "linears" not previously recognized; some lineaments were found to parallel major fault trends or regional joint sets, and thus to reflect regional tectonic patterns. Nicolais (Reference 31) reported that lineament mapping and lineament intersection-density contouring allowed the selection of target areas for mineral exploration; five of ten target areas selected independently of ground truth coincided with known mineral districts. Wier, et al. (Reference 52) reported that roof-fall hazard maps could be prepared from contour maps of Landsat lineament intersection density and spacing density. Mapping of "... supposed faults, joints and dykes, ... also alignments of drainage patterns and topographic forms and other linear tonal changes or discontinuities ..." permitted the extension of known faults and the establishment of a working hypothesis linking the occurrence of kimberlite pipes and dikes with regional, "fundamental" linear trends and the setting of criteria for locating targets for exploration (Reference 1).

2.2.2.3 Computer-Assisted Analysis

The computerized analysis of linear features in an image has taken four forms. In the first case, photointerpreted data (lineament endpoints) were digitized and summary statistics calculated by a computer (References 33 and 34). In the second case, an image was viewed by a vidicon camera and

enhanced for edge effects by an analog television system; edge effects were enhanced by producing electronically a negative image offset in the scan line direction (Reference 36). In the third form, a digital image was subjected to digital manipulation so that lineaments might be photointerpreted from obvious clues rather than from subtle clues (References 12, 18, 35 and 37). In a recent study, an image was subjected to local line detector operations which were then linked using additional algorithms to provide a final product displaying linear features (Reference 46).

Photointerpretation of Landsat images can be assisted and facilitated by computer manipulation of digital values to produce enhanced images. Goetz, et al. (Reference 12) found that mapping of lineaments from contrast-enhanced, color-composite images was useful in extending the length of known faults, in locating areas structurally favorable for the development of ground-water resources, and in detecting previously unknown faults and fracture systems. They also found a relationship between lineaments and previously mapped aeromagnetic anomalies representing offsets in basement rocks. Hoffer and staff (Reference 18) also found computer-enhanced, color-composite images to be very useful in producing maps locating lineaments and showing lineament-intersection density contours. There was a strong relationship between a large number of lineament intersections and known mineral deposits. Density contours indicated an area where mineral deposits had not been known to exist, but which subsequent field work verified to be an area suitable for detailed geologic exploration. Jackson, et al. (Reference 22) found that "the most effective enhancement procedure appeared to be the making of edge-enhanced color composites of Landsat bands and ratios." Gunther (Reference 14) suggested that a particular form of principal components analysis yielded images very suitable for lineament mapping, but no maps have been produced using this technique.

Many types of digital enhancement to emphasize linear features have been attempted. Following preliminary work done by Podwysocki, et al. (Reference 36), an initial evaluation of the image enhancement techniques was completed by Ramapriyam, et al. (Reference 37) prior to the initiation of this study. The digital image processing for the initial evaluation was accomplished on the VICAR System (Section 4.2.2) at GSFC. This processing indicted that, in practice, several of the algorithms available on the VICAR system were not suitable for enhancement of lineaments, even though they appeared promising in theory (Reference 32). Several different convolution filters were very time consuming (for both analyst and computer) and produced images that were judged inferior to simple contrast stretches for lineament enhancements. An evaluation study conducted by General Electric (Reference 6) concluded that geological scientists and engineers nearly always selected a linear stretched image as the single best image for display of lineament details. A principal component transformation also produced an unsatisfactory image.

Subsequent processing (Reference 32) indicated that the 101 x 101 pixel-size box-filter was economical and produced a useful image. This filter computes a mean value of grey levels of all pixels within a user-supplied box of dimension x and y, and subtracts this mean from the value of the pixel in the center of the box. This computation removes the low frequency value from the original picture and yields an image composed of only the high frequency components. This procedure is known as high-pass filtering. Because linear features are high frequency phenomena, they are enhanced by this procedure.

Edge detection algorithms were also tried on MSS data (Reference 32). This process requires input of intensity values for each algorithm. The input values must be fine

tuned by repeated processing and evaluating the film products. This tends to be a costly process in terms of analyst and computer time and film resources. The resultant edge images appear as white edges on black background and are difficult to interpret due to lack of identifiable landmarks in the image. Therefore procesing by this technique was not pursued any further.

In this study the Landsat-MSS/Seasat-SAR merged data were found to be more useful for lineament detection and land-cover classification than the Landsat or Seasat data alone. The actual procedure used for image contrast enhancement is described below (Section 5.3).

2.2.2.4 Appalachian Lineaments

Several remote sensing studies have dealt directly with lineaments of the Appalachian Region. Several are reviewed in detail below.

Lineaments from several sources (Landsat MSS, Skylab, Aircraft 4-channel SAR, Aircraft 12-channel MSS, and air photography) for a gas field test site (Mississippian-Devonian shales) in West Virginia have been studied (Reference 22). The test site, the Cottageville (Mt. Alto) gas field, was devoid of known surface-mapped geologic structures. In the Precambrian basement rocks, the Rome Trough extends NE-SW through the test site. Seismic studies have shown that high-producing wells are located over a steeply dipping region near the basement. Suspected fractures in the producing zone have no known surface expression; interpreted lineaments were subtle and subjective, and could not be confirmed by field investigations. Both optical and digital enhancement techniques were applied to the images, but without success in making the subtle lineaments obvious. No relationship between surface lineaments and gas production was found.

In an Appalachian Lineaments Workshop, several reports were presented on the observed relationships between linear features and oil or gas production from Devonian shale (Reference 2). Lessing from West Virginia reported that Landsat and aircaft remotely-sensed images had been found to be very useful in identifying mining hazards, karst subsidence hazards, landslide hazards and high-yield water wells, but Landsat lineaments had not yet proven to be of value in oil and gas production.

McClish and Johnson from Ohio reported some positive relationships between Landsat lineaments and field boundaries and trends; they also documented subsurface fractures correlated with a lineament (see also Reference 23).

Adams and Raymond from Kentucky reported that lineament trends did not always correspond to gas reservoir trends, but that the density of lineaments appeared to be an indicator of gas production.

Gathright, Webb and Millici from Virginia reported that aircraft lineaments with a strong NW trend were missing from Landsat images and lineament maps (Sun-angle problem).

O'Farrell from Tennessee reported that a Lineament Intersection Cluster Map (LICM) had been prepared and compared with existing oil and gas data to target areas for further exploration; this is based on evidence that greatest production of gas comes from wells where many fractures intersect.

Dr. Alexander from Pennsylvania reported that there was some correspondence between the orientation of lineament sets and the shape of oil- and gas-producing fields; he also repeated the suggestion that major lineaments correspond to zones of increased fracture permeability, and that movements along these lineaments "... may have provided fundamental structural controls on the deposition and accumulation of hydrocarbon deposits..."

Van Tyne and Wickerham from New York noted some correlation in local areas between lineament data and oil or gas field locations. These preliminary reports gave indications of the utility of lineament analysis in the Appalachian Region.

In a study sponsored by the Appalachian Regional Commission (see Section 3), Johnson (Reference 23) compared Landsat lineaments with various types of ground truth. He found that there was a significant correlation between "... Landsat lineaments and the boundary and extension of several gas or oil fields." Lineaments drawn from multiseasonal enhanced images were found to have ground expression, both in the form of surface physiography and in the form of joint and fracture density and orientation trends, with associated increased water flow. Johnson concluded that "... Landsat lineaments are potential tools to enhance gas production by locating zones of higher permeability due to fracturing and joints in Devonian Shale."

A statistical study of the distance relationships of producing gas wells (Devonian shale) with respect to lineaments has been conducted in West Virginia (Reference 56). Simple and multiple linear regression equations were fitted in a stepwise manner to First Year Average Daily Production (FYADP) data for 40 wells located in Lincoln County and Wayne County (dependent variable), to the location of each well with respect to lineaments and lineament intersections detected on U-2 images, and to lineament length (independent variables). Predicted values, based on the derived regression equation, for 9 new wells located within acceptable limits of lineaments matched closely actual recorded values for those wells. The authors concluded that the regression models were useful for choosing well sites with highest predicted productivity, based only on lineament parameters.

SECTION 3 - STUDY AREA

The study area of this report is part of a study area used by the Appalachian Regional Commission (ARC). One of the commission's functions is to coordinate efforts in mineral resource exploration and exploitation (particularly hydrocarbons). The commission supports mapping regional and local fracture systems that might control mineral deposits, detecting surface alterations possibly associated with mineral deposits, and providing basic data for geologic mapping. One of the commission's study areas covers parts of three states--West Virginia, Ohio, and Kentucky--and is approximately centered where the three states intersect near Huntington, West Virginia.

Within the area mentioned above, the study area described in this report is located between latitudes of 38° $13'$ North and 38° $40'$ North and between the longitudes of 82° $00'$ West and 82° $35'$ West. The study area covers Cabell County, parts of neighboring counties in West Virginia, and neighboring parts of Ohio. The study area is shown in Figure 3-1 as shaded portion.

The area, which is approximately 10,000 square km, is part of the Cumberland plateau. Local relief on the plateau varies by approximately 400 feet. The highest point is 945 feet in elevation and the lowest approximately 540 feet (the Ohio River).

The area is mostly covered with forests but there are small areas where agriculture is developed. Flat areas are found only on the narrow flood plains of the Ohio River and fossil Pleistocene drainage systems. Examination of the images shows that lineaments are well expressed on Landsat images because of the tonal contrast enhancement due to the Sun's oblique illumination, the suppression of distracting spatial

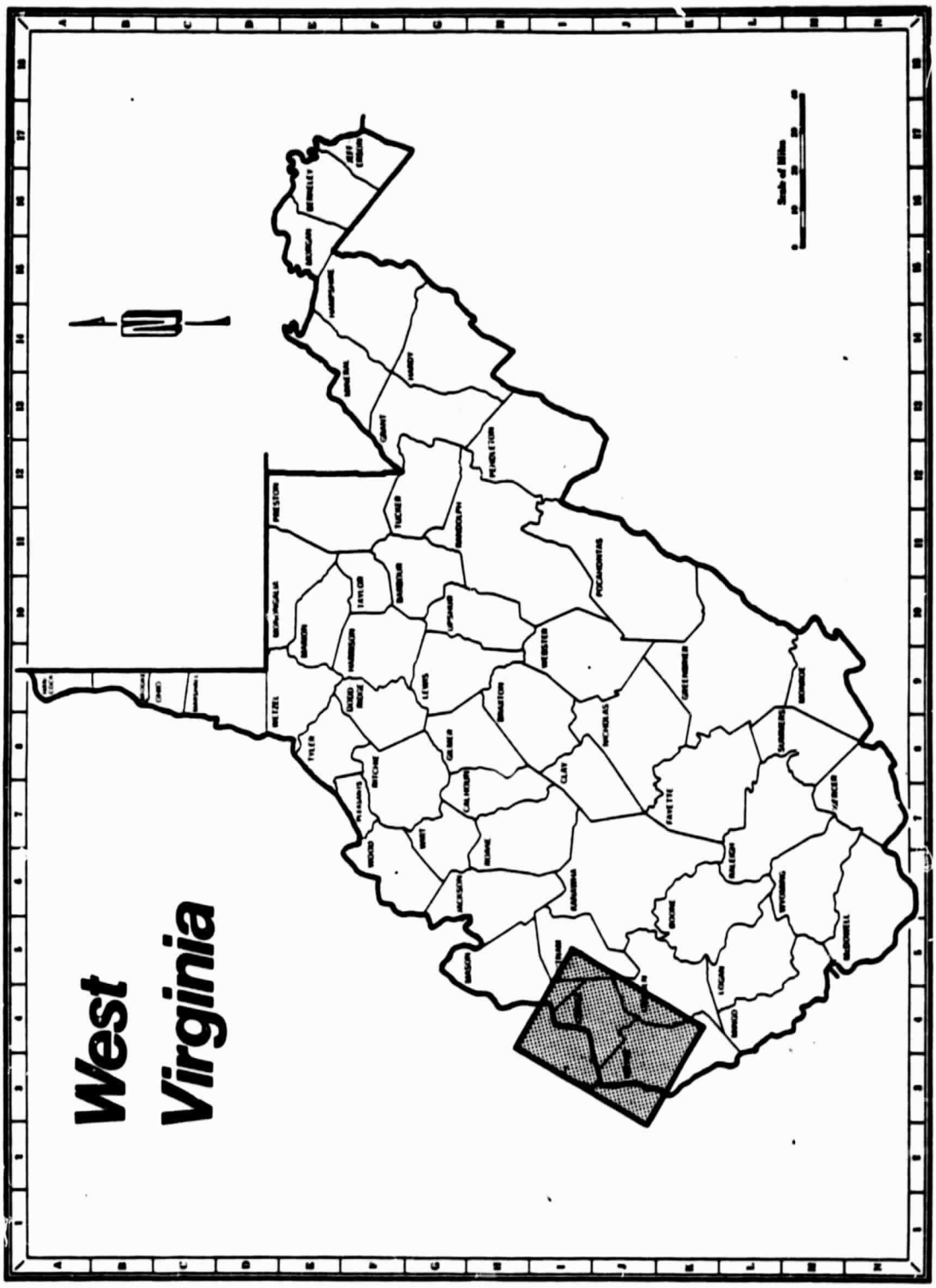

Figure 3-1. Lineament Study Area

details resulting from coarser resolution than that of high-altitude aerial photographs, and the regional coverage of the satellites. Similarly, the oblique illumination of the radar beam produces a highlight and shadow effect which increases the tonal affects in the Seasat imagery, which consequently, enhances the lineaments in a radar image.

The 38th parallel lineament (Reference 16), a 3000 km-long, highly variable linear structural feature, passes a little south of the study area. The presence of local rather than regional lineaments within the study area may be assumed from the known density of local lineaments for the Appalachian plateau (Section 2.2.2.4).

SECTION 4 - DATA

4.1 ACQUISITION AND CHARACTERISTICS

Three types of remote sensing data were used in the study: four channel Multispectral Scanner (MSS) Landsat data, Seasat-1 Synthetic Aperture Radar (SAR) data and Landsat/ Seasat merged data. Images covering the study site and immediately surrounding areas were extracted from larger images. MSS bands 4, 5, and 7 were digitally enhanced and projected through blue, green and red filters to form the Landsat color composite (Figure 4-1). The Seasat-1 SAR image was linearly stretched to produce the Seasat black and white image (Figure 4-2). Other information regarding the Landsat and Seasat images is given in Table 4-1.

Two Landsat scenes, one with identification number 2908/15083 for July 18, 1977 and the other with identification number 30067/15302 for May 11, 1978, were used. The Landsat scenes have the standard (Reference 11) Landsat data format and were acquired from the Goddard Space Flight Center. The July 18 Landsat data were merged with Seasat data. Details of geometric correction, registration and merger of the two data sets are described later (Section 5).

The Seasat-1 scene for August 27, 1978 was provided by the Jet Propulsion Laboratory (JPL), California. The Seasat data were digitally corrected and were on computer compatible tape (CCT). The data were processed on the JPL Interim Digital Processor, from raw data supplied by the JPL Seasat Data Utilization Project. The tape contained one Seasat-1 SAR image frame which covers an area of approximately 100 x 100 kilometers. The header information pertaining to the tape received from JPL is given in Table 4-2.

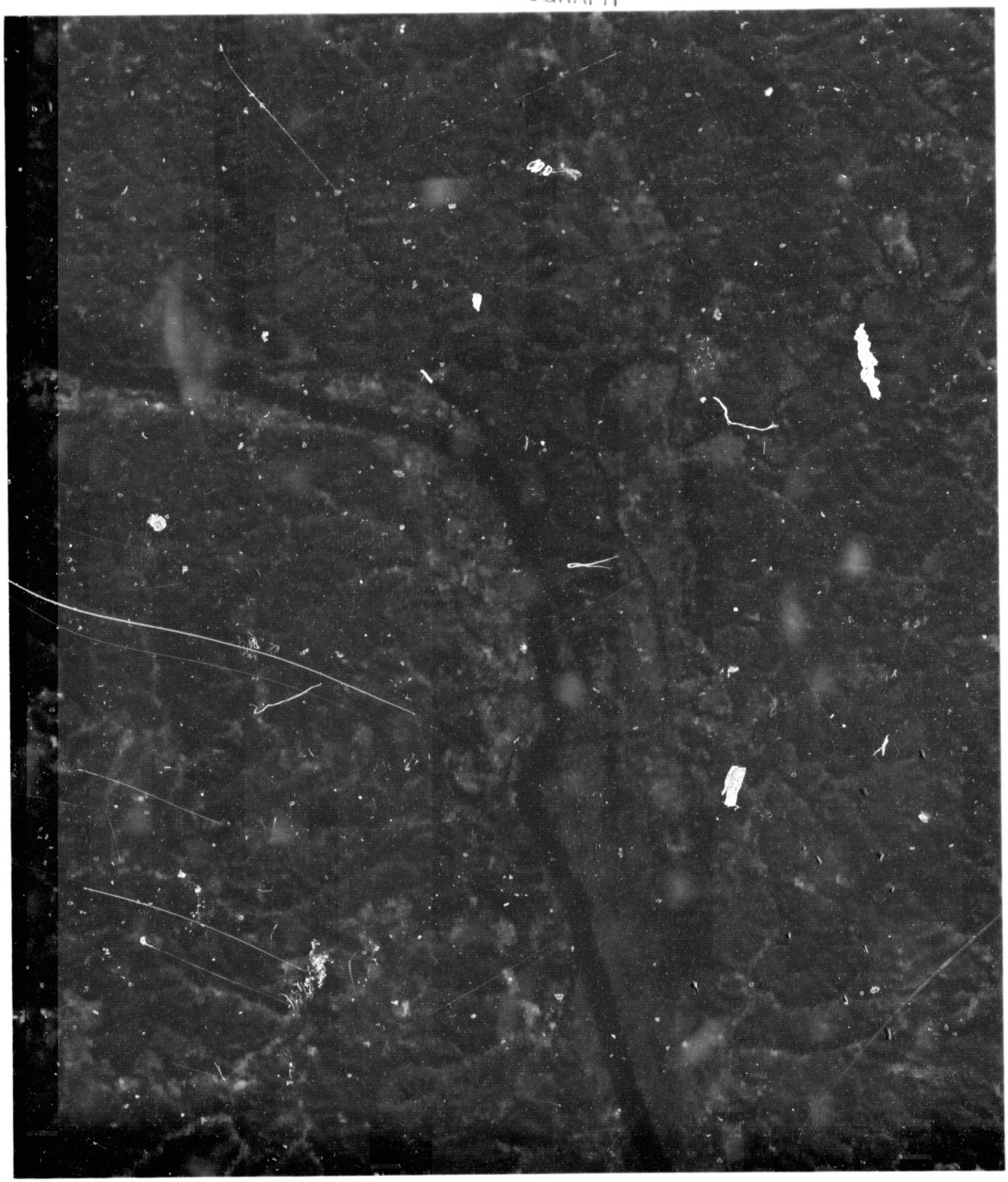

Figure 4-1. Color Composite of July 18, 1977 Landsat Enhanced Image

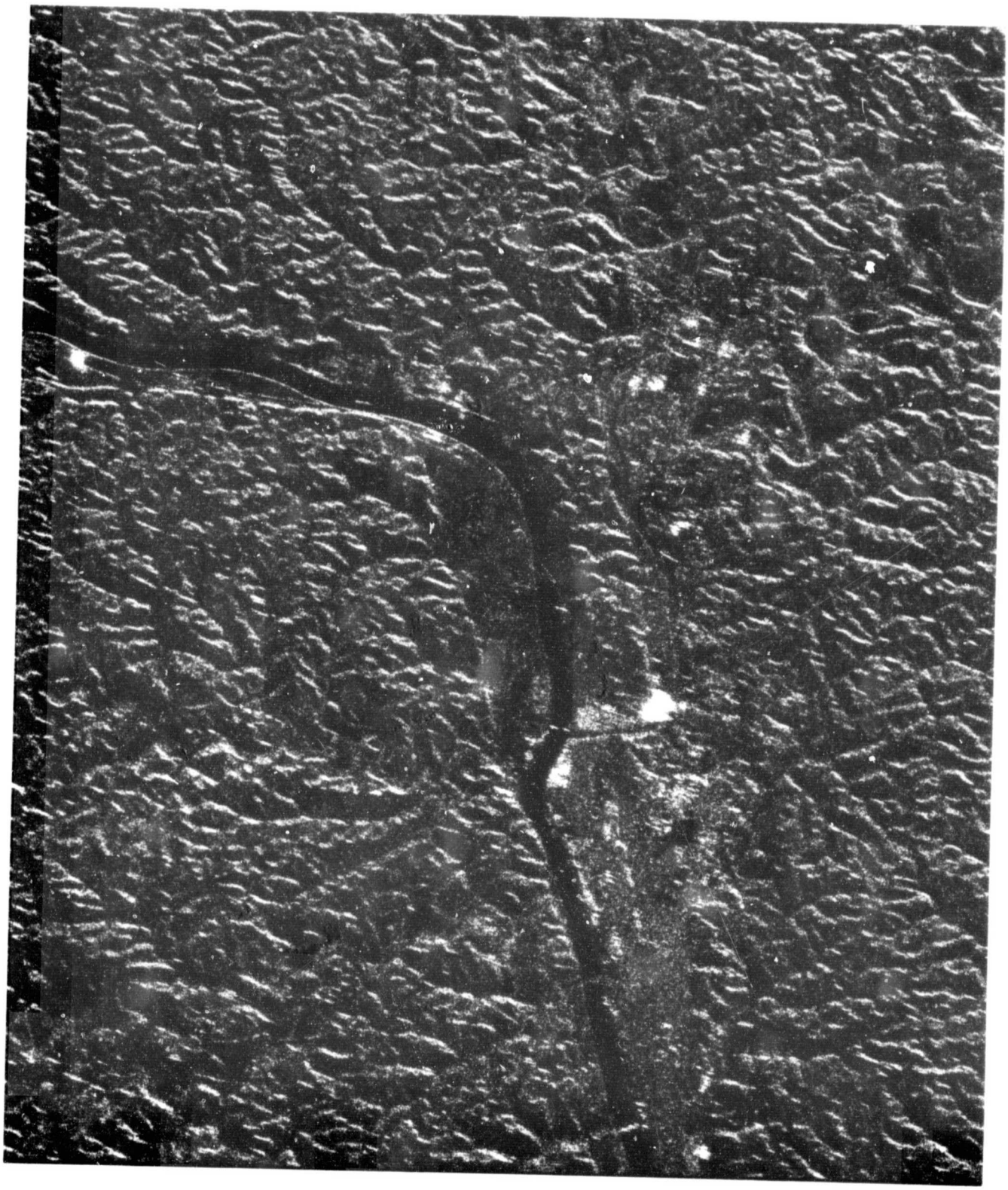

Figure 4-2. August 27, 1978 Seasat Enhanced Image

Table 4-1. Center Coordinates and Sun Elevation Angle or Look Angle for Landsat and Seasat Scenes

Scene	Center Coordinates North	West	Sun Elevation Angle Or Look Angle
Landsat MSS:			
July 18,77	38° 45'	82° 43'	57°
May 11,78	38° 45'	82° 32'	57°
Seasat SAR:			
Orbit 874			
Aug. 27,78	38° 22'	82° 34'	Near range 19.5°
			Center range 23.1°
			Descending track heading 202.7°
			(North = 0°)

Table 4-2. Seasat (SAR) Computer Compatible Tape Header Format

Title	:	JPL digitally processed in Seasat Radar image
Data tape ID code	:	08740025
Frame starting time	:	239:02:57:05
Station ID	:	MIL
Date processing data	:	16 June 1979
Processing run	:	1
Latitude of target area	:	$38^{\circ}\ 22'$ North
Longitude of target area	:	$82^{\circ}\ 34'$ West
Site	:	Kentucky
Number of Samples/line	:	6144
Total number of lines	:	5840
Pixel spacing in azimuth	:	16 meters
Pixel spacing in range	:	18 meters
Resolution in azimuth	:	25 meters
Resoltion in range	:	25 meters

The Seasat-1 SAR image resolution is approximately 25 meters by 25 meters. The pixel spacing is approximately 16 meters along track and 18 meters cross track. The image record direction is approximately north to south for a descending path and south to north for an ascending path. Each pixel value is an 8-bit encoding of the reflected amplitude averaged over 4 independent looks. The average pixel value is approximately 40 (digital value) over a possible range between 0 and 255. This provides ample dynamic range to record the highly reflective (bright) targets. Radiometric compensation for the radar gain control, which varies over the swath width and can be compensated for in the image domain, was not applied.

The computer compatible tapes (9 track, 1600 BPI CCT's) produced by the SAR digital processor have two types of records. These are the header record and the data line records. Each record on the tape consists of 6144 bytes. The tape format is shown in Figure 4-3 (reproduced from Reference 55). In the figure, one 'TM' designates a tape mark indicating the end of a file and the start of a new file. Two 'TM's designate the end of last file on the tape. Normally a data tape contains a single file corresponding to one 100 km x 100 km Seasat image.

The first record in a file is the header record (Table 4-3 reproduced from Reference 55). The values in items 1 through 9 are in character format and are left justified. The values in items 10 through 15 are in integer format.

Each data line contains 6144 samples. If there are less than 6144 pixels in a line, an appropriate number of zeros is inserted at the end of each data line record. A typical image file contains approximately 5500 data lines. Each pixel is represented by one 8-bit binary byte having a value

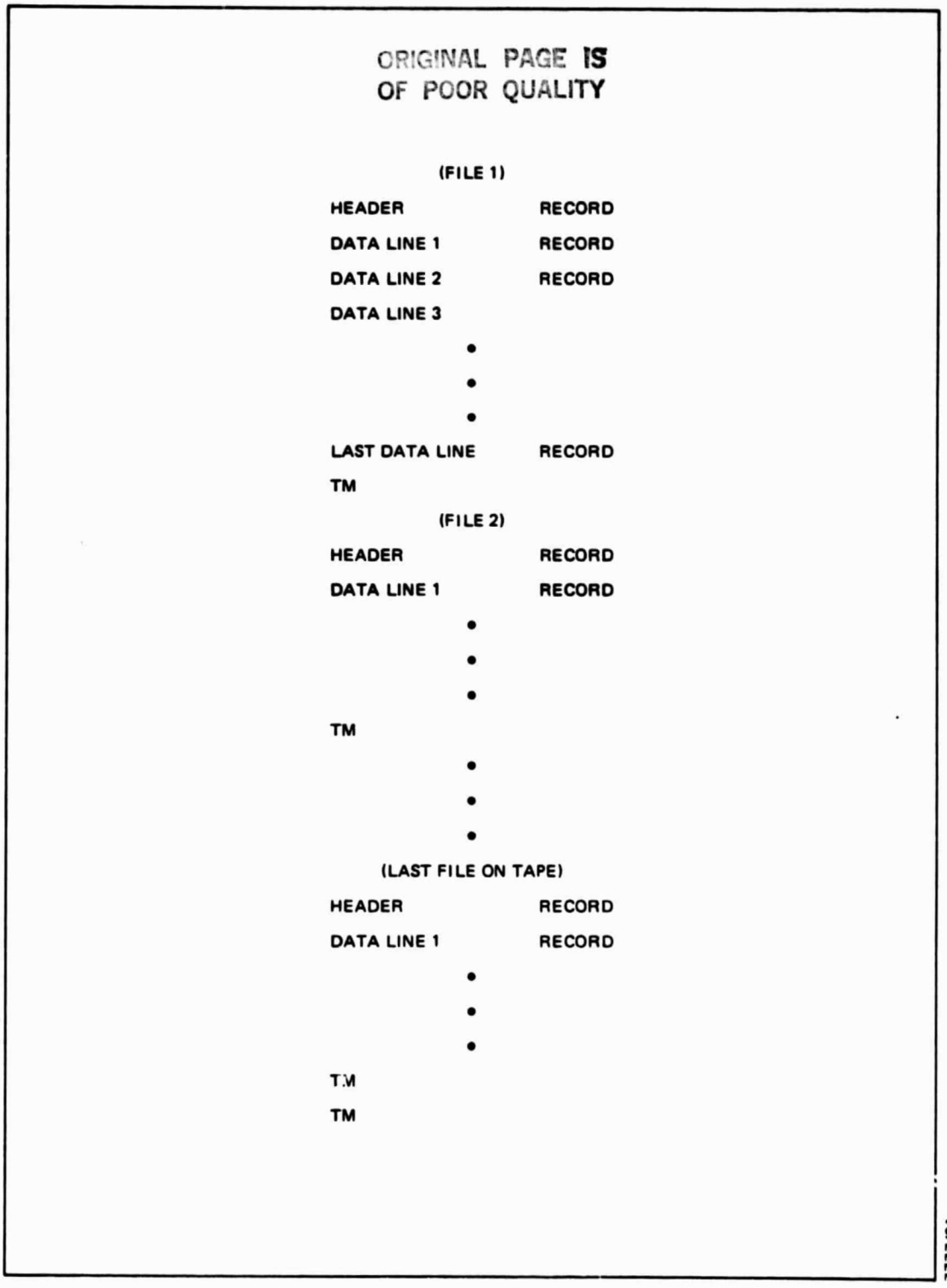

Figure 4-3. Seasat Image Computer Compatible Tape Format

Table 4-3. Seasat Data Tape Header Record Format

ITEM	DESCRIPTION	BYTES	LOCATION	REMARKS
1	TITLE: 'JPL DIGITALLY PROCESSED SEASAT RADAR IMAGE'	44	1-44	
2	DATA TAPE ID CODE: XXXXYYYY	8	45-52	XXXX = ORBIT NUMBER (REV) YYYY = TAPE NUMBER
3	FRAME STARTING TIME: DDD:HH:MM:SS	12	53-64	ACTUAL TIME OF DATA TAKEN
4	RECEIVING STATION IDENTIFICATION: SSS	4	65-68	WHERE SSS IS THREE CHARACTERS OF STATION ID: ULA = ALASKA GDS = GOLDSTONE MIL = MERRIT ISLAND UKO = OAK HANGAR SNF = SHOE COVE
5	PROCESSING DATE: DA-MON-YR	12	69-80	
6	PROCESSING RUN: RRRR	4	81-84	RRRR = PROCESSING RUN NUMBER (BEGINS WITH 1)
7	LATITUDE OF TARGET AREA: XXX:YY:N (OR S)	8	85-92	XXX = DEGREE YY = SECOND N = NORTH S = SOUTH
8	LONGITUDE ON TARGET AREA: XXX:YY:W (OR E)	8	93-100	XXX = DEGREE YY = SECOND W = WEST E = EAST
9	SITE: (NAME OF TARGET AREA)	24	101-124	
10	NUMBER OF SAMPLE/LINE N_S	2	125-126	N_S <6144
11	TOTAL NUMBER OF LINES N_L	2	127-128	N_L <6144
12	PIXEL SPACING IN AZIMUTH M_A	2	129-130	TYPICALLY ≅ 16 METERS
13	PIXEL SPACING IN RANGE M_R	2	131-132	TYPICALLY ≅ 18 METERS
14	RESOLUTION IN AZIMUTH R_A	2	133-134	TYPICALLY 25 M
15	RESOLUTION IN RANGE R_R	2	135-136	TYPICALLY 25 M
16	BLANKS	6008	137-6144	

7777/81

in the range from 0 to 255. Seasat-1 SAR characteristics are given in Table 4-4.

4.2 PROCESSING SYSTEMS

Processing of MSS and SAR images was achieved through the use of the Eastern Regional Remote Sensing Applications Center's (ERRSAC) Interactive Digital Image Manipulation System (IDIMS) (Reference 9), and the Video Image Communications and Retrieval (VICAR) system developed at the Jet Propulsion Laboratory (JPL) (Reference 30). Brief descriptions of the two systems follow.

4.2.1 IDIMS

IDIMS is a mini-computer based image processing system configured by Electromagnetic Systems Laboratory, (ESL) Inc., of Sunnyville, California. IDIMS software is used to reformat, enhance, geometrically correct, classify, and produce output products of Landsat MSS and other remotely sensed digital data. The IDIMS system hardware configuration along with other supportive software available at ERRSAC is illustrated in Figure 4-4 (Reference 4).

A typical analysis sequence for processing Landsat or other digital image data using IDIMS is as follows. The Landsat CCT, which is available either at 800 bits per inch (bpi) or 1600 bpi recording densities (IDIMS accepts only the latter), is acquired. The data are reformatted and read onto a disk. Then geometric corrections are performed to orient the data to true North and match it to a map projection. Images can be classified for landcover type by the analyst using supervised techniques (classification of images using statistics developed from small training sites containing distinct spectral properties and representing distinct landcover types) or unsupervised techniques (classification of digital images by categorizing pixels into groups of similar spectral characteristics without the aid

Table 4-4. Seasat-1 SAR Characteristics

SATELLITE ALTITUDE	800 KM
RADAR WAVELENGTH	23.5 CM (L-BAND)
FREQUENCY	1.3 GHZ
PULSE REPETITION FREQUENCY	1463 TO 1640 PPS
PULSE WIDTH	33.1 MICROSECONDS
NUMBER OF LOOKS	4
PEAK TRANSMITTED POWER	1000 WATTS
POLARIZATION	HH
DATA RATE	110 MBITS/S
SWATH WIDTH	100 KM
RESOLUTION	25 X 25 METERS
INCIDENT ANGLE ON THE SURFACE	23° ± 3° ACROSS THE SWATH
INTEGRATION TIME	2 SECONDS (4 LOOKS)

7777/81

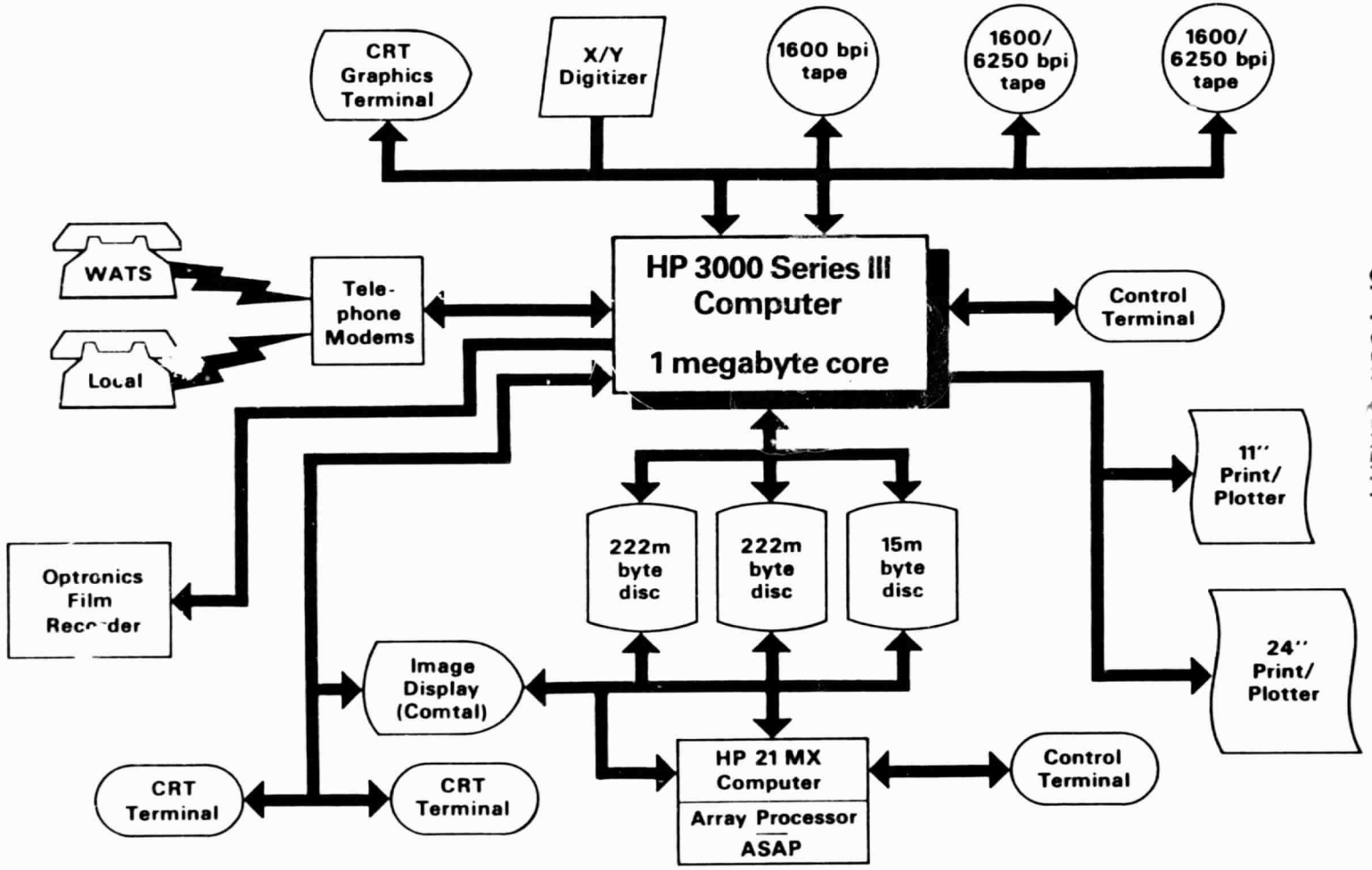

Figure 4-4. The IDIMS System Hardware Configuration

of training-site data). Statistical manipulation or further class refinements can also be performed on the system. Several other functions, including various image enhancement techniques, can be performed on the system. Output products can be generated via line printer, electrostatic plotter, or film recorder. These products can be in statistical, tabular, graphic, or image format.

4.2.2 VICAR

A batch version of the VICAR system, originally developed at the Jet Production Laboratory (Reference 30), is operational at the Goddard Space Flight Center (GSFC). It is designed to provide the analyst with an efficient system of recording, processing, and displaying pictures; it is also used for algorithm development. The system library consists of about 100 executable programs, some of which were provided by JPL and others of which were designed and implemented at GSFC. The system uses a high level, problem-oriented language and an automatic data-handling system. The automatic data-handling system uses a standard format for both disk and tape data sets. All system programs are designed to operate with this standard format. An internal processor is available to convert various tape formats to the standard format. The final product from the VICAR system is saved on tape and the photoproducts, if any, are produced on some other system such as DICOPAK (Reference 47).

SECTION 5 - VISUAL ENHANCEMENT OF LINEAMENTS

The Seasat-1 SAR data was the primary source for finding lineaments in this study. Two additional data sets, Landsat data and Landsat data merged with Seasat data, were used as supplementary information. In this study several computer analysis techniques were used on the imagery to make the linear features more obvious. A brief summary of the experience gained on the number of enhancement techniques used for lineament study is given below.

5.1 GEOMETRIC CORRECTION AND REGISTRATION

To assure correspondance of the different images of the target area, all three images (Section 4.1) were registered to a common base, using USGS 7.5 minute quadrangle topographic maps of the area. Geometric corrections like pixel squaring and corrections for skew and rotation were achieved through registration. The procedure for registration is given below.

Registration was achieved through the use of ground control points (GCPs). GCPs are points that can be accurately located both in an image and on a map. A computer program calculates the relationship between the map GCP coordinates and image GCP coordinates. Transformation coefficients are determined by performing a least squares fit on the GCPs. Another computer program performs the reformatting and resampling of the image based on the transformation coefficients. Registration was accomplished in several steps (Figure 5-1).

Image GCP's were selected by displaying the Landsat data on the IDIMS digital display and interpreting the significant landmarks that could be matched with known map locations throughout the image. The line and sample values were saved in a mensuration file. These landmarks were paired with the corresponding features on the area map (1:24,000 scale) and

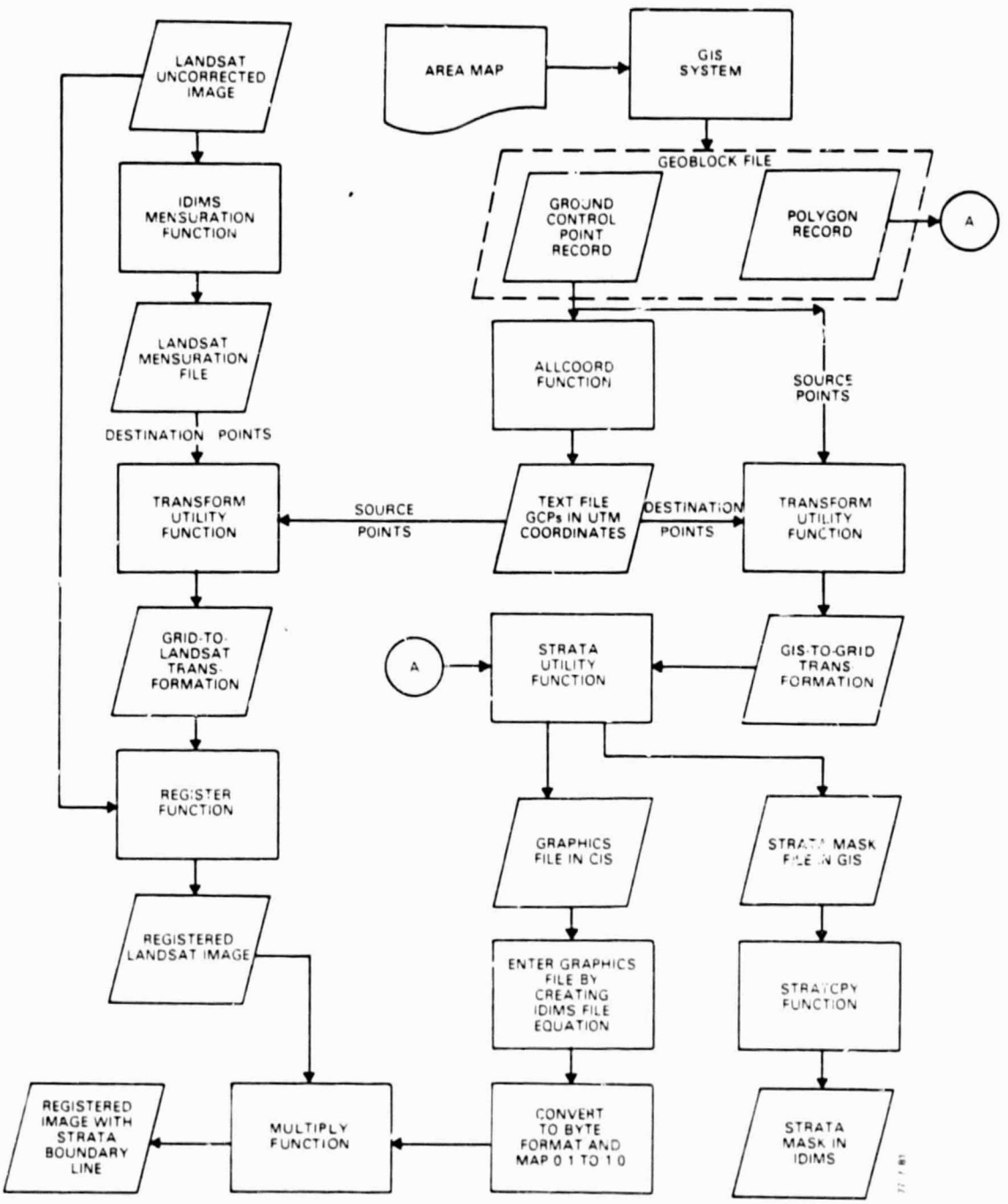

Figure 5-1. Functional Diagram for Image to Map Registration and Creating Strata Mask and Graphics Overlay

the points marked on the map with identifying labels. ERRSAC's Geographic Entry System (GES) (Reference 45) was used to create the corresponding GES ground control points file (also known as geoblock record) by digitizing the locations of the points from the area map. Another GES file was prepared to delineate the Cabell County line.

The July 18 Landsat image was first registered to a Universal Transverse Mercator (UTM) projection and subsequently all the other images were registered to the July 18 image. Data from a large area (715 lines by 1024 samples (columns)) were processed to allow for positional error and control point selection. All subsequent control point selection was performed on this subsection.

The more technical details of the registration process are given below. The geoblock record of ground control points is input into the IDIMS ALLCOORD function to create a text file for GCP's in 50-meter grid Universal Transverse Mercater (UTM) coordinates. This text file is then read into the TRNSFORM utility function to provide source points* and the image mensuration file as destination points*--generating Grid-to-Landsat transformation for registering the uncorrected Landsat image. The text file produced earlier is then used as destination points and the GES geoblock control point record is used as source points for the TRNSFORM utility function to generate GES-to-Grid transformation. This transformation, along with line and polygon

*The IDMIS function REGISTER calculates an inverse transformation by mapping the output image ("source") to the input image (destination). Thus one must use reverse logic to do registration in IDIMS. The IDMIS function STRATA does the opposite and maps the source to the destination.

geoblock record is input into the IDIMS STRATA utility function to generate graphics and a strata mask file. The strata mask file is input into IDIMS STRATCPY function to generate a strata mask. The graphics file must be entered into IDIMS as an image by creating a file equation. In IDIMS, the image format is converted to byte format and the new image containing only values of 0's and 1's is mapped from 0 1 to 1 0. At this stage the political boundary lines will have a value of 0 and the remainder of the image having a value of 1. The graphics image is then multipled by the registered image. The line data (having a value of zero) will retain a value of zero in the output image and will display as black in the new image. The resulting image therefore outlines that part of the image covering the study area, but contains data both within and without.

In the case of image-to-image registration, one of the images must have been previously registered to the map so that the new image is also registered to the map. Both the May 11 Landsat MSS image and the Seasat SAR image were registered to the July 18 Landsat MSS image. Mensuration files containing ground control information were then created for the May 11 Landsat MSS image and Seasat SAR image and they were used as destination points in the respective transformation function. The July 18 mensuration file was used as the source point file. The transformation equations thus developed were used to register the May 11 Landsat MSS image and Seasat SAR image to the July 18 Landsat MSS image. The resulting registered images were 1024 x 1024 pixels with a 50 x 50 meter pixel size.

The registered images were then multipled by the strata mask image to get an image containing Cabell County alone. The strata mask image contains only 0's and 1's, zero's outside the strata boundary and one's inside the boundary. Thus

multiplying an image by the strata mask image eliminates all the pixels outside of the boundary. Pixels inside the boundary are retained without any change. The new image size was 840 lines and 810 samples without any change in pixel size. This masking was performed to produce images containing data only for that part of the image covering the study area. The image was used as input to generate the final classification products.

5.2 IMAGE CONTRAST ENHANCEMENT PROCEDURE

Previous work (Section 2.2.2.3) showed that advanced image enhancement techniques, such as edge detection and Log Box filtering were not optimum for enhancement of lineaments. Other techniques such as Box filtering, addition of a Box-filtered image to an original image, were also found inferior to linear or piecemeal stretch enhancement (Reference 32).

A linear contrast stretch was applied to the Seasat and Landsat images to enhance them. This procedure increases image contrast, which causes certain features to stand out more clearly. The original range of digital values is expanded to utilize the full range of the recording film or display device (a brightness range from 0 to 255 (0 represents black and 255 represents white). In general, each of the four MSS bands has a range of about 50 grey levels or less and must be stretched to occupy the full range from 0 to 255 to attain maximum tonal contrast. The Seasat-1 SAR data has a majority of the values in a range of about 80 grey levels with a mean at about 40. Few of the pixel values (less than 5 percent) are much larger than the upper limit of this range. For digital contrast and edge enhancement details, the reader is referred to any textbook on remote sensing or to Wescott and Smith (Reference 49).

IDIMS has two functions for increasing the contrast of images. The SCALE function linearly stretches the data between specified percentage limits for saturation of black and white tones. These percentages can generally be varied from 0 to about 3 for each end of the spectrum. If part of the image is blank (contains zeros), the lower limit must be padded with a percentage representing the blank portion of the image. Geometrically corrected images sometimes have such blank portions. A simple histogram will show exactly what percentage of the image is blank. The IDIMS function MAP can either stretch the image piecewise or linearly between two or more specified grey levels. The lower and the upper grey level limits for the resulting stretched image are specified and may be different from 0 and 255.

The VICAR function ASTRETCH2 is similar to SCALE, but an option exists which specifies an F-times stretch about the histogram peak. F is a real constant between 1.0 and 128.0. The Seasat SAR image was enhanced using this function with a F value of 3. Other values of F produced images with inferior contrast. The Landsat images were enhanced using IDIMS functions.

5.3 LANDSAT/SEASAT DATA MERGE

Landsat imagery has been used extensively for lineament mapping by a number of investigators (Section 2.2.2). It is the intention of the author to demonstrate the superior applicability of Seasat-1 SAR imagery for lineament mapping. In our effort Seasat SAR data was the primary data base while the merged Landsat-MSS/Seasat-SAR data was used for comparison. The two data sets were merged in the following manner:

1. The first step was to register the Landsat MSS and Seasat SAR images to a common base as described in Section 5.1. The Landsat data base used for merger was

Scene 2908.15083 for July 18, 1977, which was registered first of all to the area map. The Seasat SAR image was registered to the Landsat MSS image. The image registrations were examined and found to be of good quality with less than one Landsat pixel error.

2. The two images, Landsat MSS with four bands and Seasat SAR with one band, were then merged, generating a five-band image. The merged data were used for landcover classification as will be discussed later (Section 6).

3. One problem existed with the use of the five-band image. An even number of bands were required for processing an image on the IDIMS system using a floating point advanced scientific array processor (ASAP) which permits very fast image computation, such as the multispectral classification. To get the required even number of bands, a sixth band was created. The sixth band was generated by taking the ratio of Landsat MSS band 7 to band 5 and scaling the ratio data to the full range of the display, 0 to 255. The steps involved in this are shown in the functional diagram (Figure 5-2) for Landsat/Seasat data merge. The sixth band was used only as a reference in the analysis and evaluation steps. The band ratio does not add new information, but a ratio describes the positive covariance information between two channels. Furthermore ratioed data of two normal distributions results in data which are not normally distributed. Hence a non-parametric classifier may be more appropriate with the ratioed data than the maximum-likelihood decision rule used here.

Extreme care must be taken in scaling the ratio band. The real-format ratio image should be mapped to an output range of 0-255 before it is converted to a byte-format image. This is done to preserve the maximum number of grey levels.

The merged data were produced in the form of a color composite hardcopy to be used for lineament mapping. For the MSS data, bands 4, 5 and 7 were used as blue, green and red images to create a standard color composite. Including the Seasat SAR band as one of the color images gave very poor results. An already-tested technique developed (Reference 8) to merge MSS and RBV Landsat data was used to produce the blue, green and red images from MSS bands 4, 5 and 7 and the Seasat SAR band. The blue, green and red images are produced in the following manner.

$$\text{Blue image} = \frac{(\text{MSS Band 4} \times \text{SAR})}{4 + 5 + 7}$$

$$\text{Green image} = \frac{(\text{MSS Band 5} \times \text{SAR})}{4 + 5 + 7}$$

$$\text{Red image} = \frac{(\text{MSS band 7} \times \text{SAR})}{4 + 5 + 7}$$

These ratioed color images are real in format and have very compressed histograms. These real images must be properly mapped before they can be converted back to byte format, so that the whole range of values may be preserved. The reasons for this were discussed above. The functional diagram describing how the ratios are calculated is essentially the same as shown in Figure 5-2 for creation of the ratio band. A color composite was produced using the blue, green and red mapped images. The Landsat/Seasat merged data color composite is shown in Figure 5-3.

5.4 LINEAMENT MAPPING

Visual procedures were used in mapping the lineaments from the enhanced Seasat-1 SAR images. An enhanced Landsat image, a Landsat/Seasat merged image and a Landsat Band 7 to Band 5 ratio image were used for feature reference and for supplementary information; these data were useful in doubtful situations. The Seasat SAR image was enlarged to

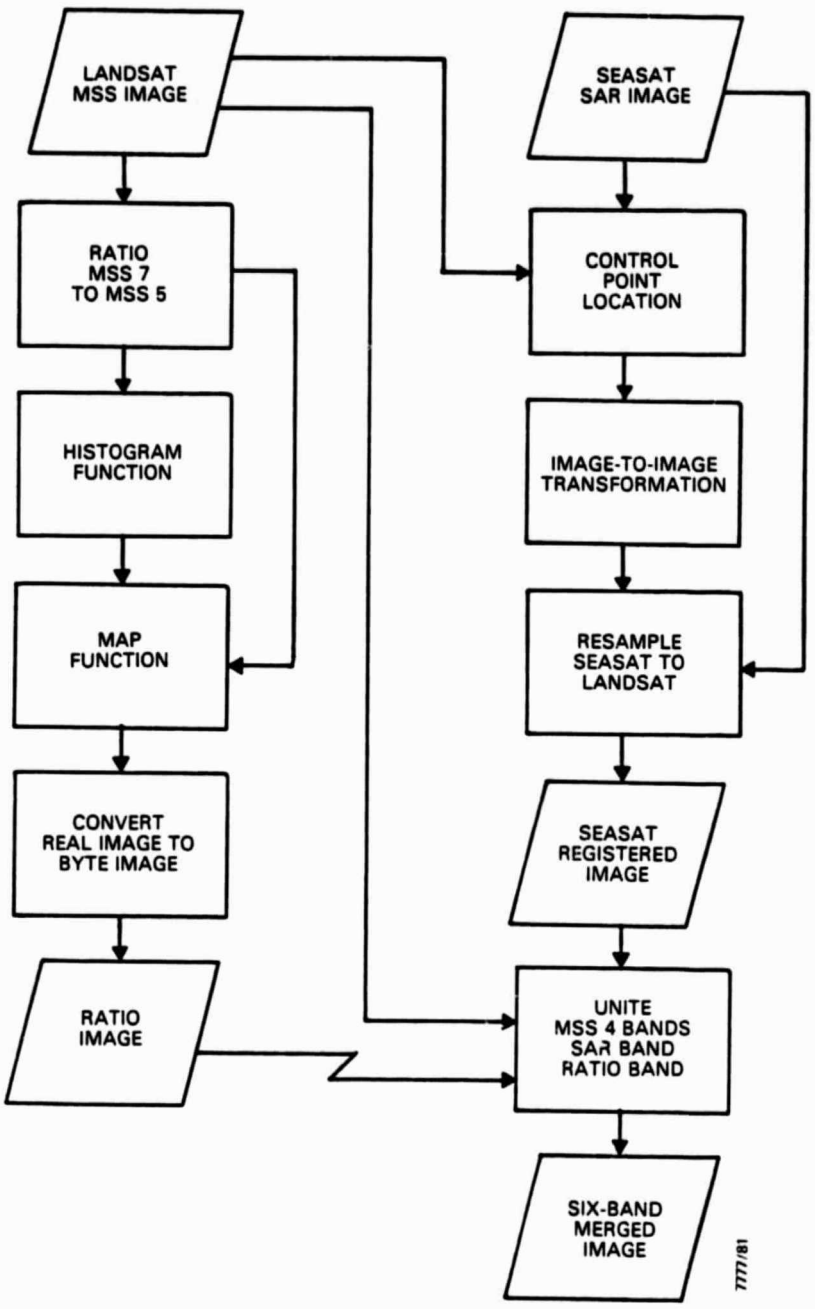

Figure 5-2. Functional Diagram for Landsat/Seasat Data Merge

Figure 5-3. Landsat/Seasat Merged Data Color Composite

1:250,000 to correspond to the available Landsat-derived lineament map for West Virginia. Lineaments were hand-drawn on a clear plastic sheet placed on top of the Seasat-1 SAR image. A diffuse light table was used for improved visibility. Artwork was performed later to create a smooth overlay. The lineament map derived from Landsat MSS images by other investigators (Reference 50) for a different purpose was not used as a reference while the lineaments were being drawn so that the comparison between the Landsat MSS and Seasat SAR derived lineaments would be objective. Figure 5-4 shows the functional diagram of lineament enhancement and mapping system.

Two viewing methods were used as recommended by Werner (Reference 48):

1. Close inspection with a line-of-sight perpendicular to the area being viewed, which is called the normal viewing method, and
2. Viewing from a low angle or a distance from the area being viewed.

He observed that method one produces shorter lineaments than method two. Werner further observed that for the Appalachian region, the first method will produce a map which correlates with the smaller geological structures, while the second method will produce a map that correlates fairly well with features of regional scale.

In the author's opinion, the direct use of merged data for lineament mapping may be very useful, but merged data were not used here because only a comparison of lineaments derived from Landsat MSS and Seasat-1 SAR was intended. Lineaments derived from Landsat MSS images for the target area were already available from the lineament map for the State of West Virginia (Reference 50). The Landsat lineament map for the target area was reproduced from the state map and is

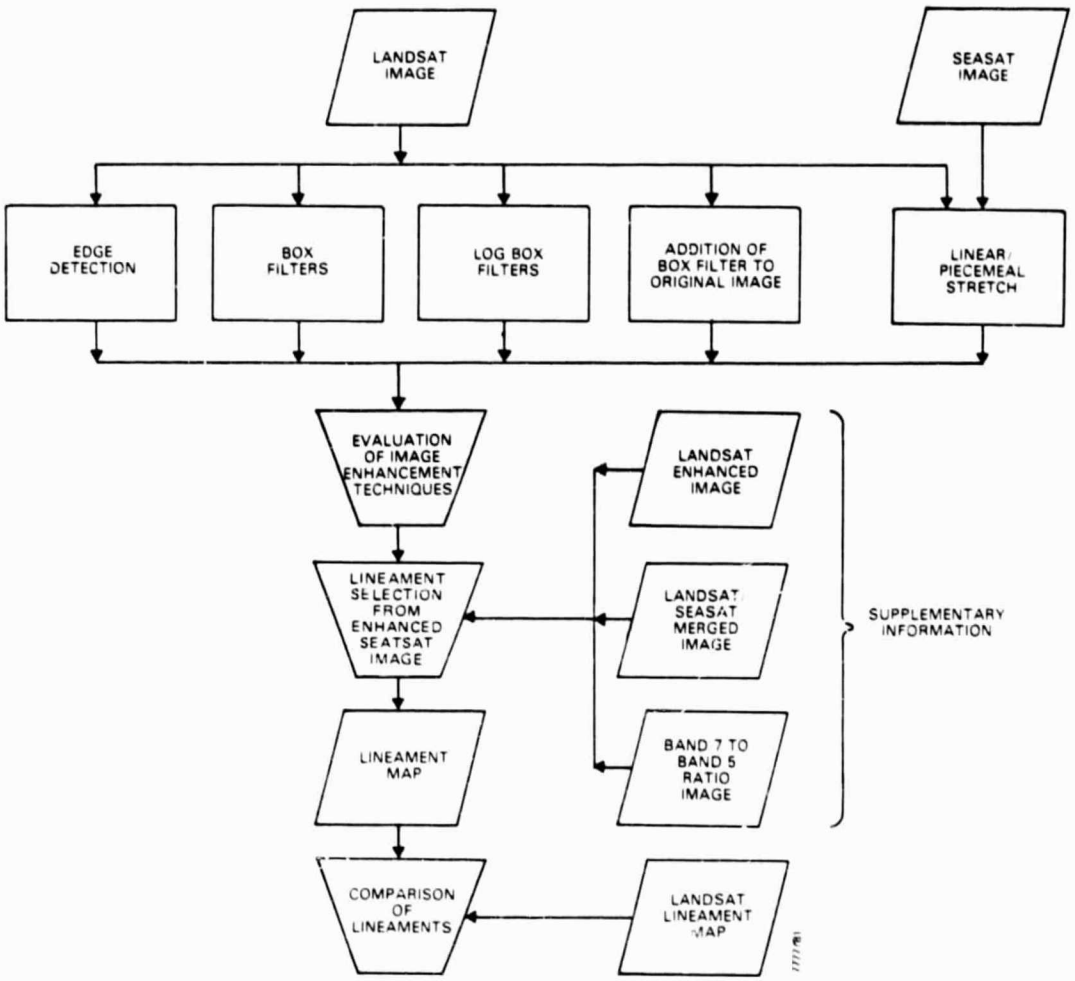

Figure 5-4. Functional Diagram of Lineament Enhancement and Mapping System

shown in Figure 5-5. The Seasat SAR lineament map for the same area is shown in Figure 5-6.

The final copy of the Seasat SAR lineament map was drafted to display lineament comparisons. Three different line configurations were used for the Seasat SAR lineaments: a solid line indicates the lineaments which match with the Landsat lineaments; a dashed line indicates the lineaments which were detected in the Seasat image but were not reported in the Landsat lineament map; a dash-dot line indicates the lineaments which were missing in the Seasat image but were reported in the Landsat lineament map. Only minor lineaments or parts of lineaments were found to be in the Landsat lineament map and missing from the Seasat SAR lineament map. It was estimated that six percent of lineaments (based on straight lineaments by number) were missing and about twenty percent new lineaments were found by the Seasat SAR mapping. The net gain of additional lineaments is about 14 percent. Significantly improved results were reported by Ford (Reference 10). He found that the number of minor lineaments mapped from the SAR images were greater than the number mapped from the corresponding MSS image by a factor of about two.

The straight Seasat-1 SAR lineaments were digitized and statistically analyzed. The locations of both ends were digitized, giving starting and ending points, thus completely representing the lineaments in a two-dimensional coordinate system. The three types of lineaments were digitized separately. Each set of digitized data was input into the Lineament-Plotting System (Reference 33) to get Rose diagrams. Rose diagrams by county are available for the Landsat lineaments (Reference 25). Rose diagrams for the matching Seasat SAR lineaments and the Landsat lineaments from Cabell and Wayne Counties are shown in Figure 5-7. The Seasat SAR lineament Rose diagram includes Cabell county and

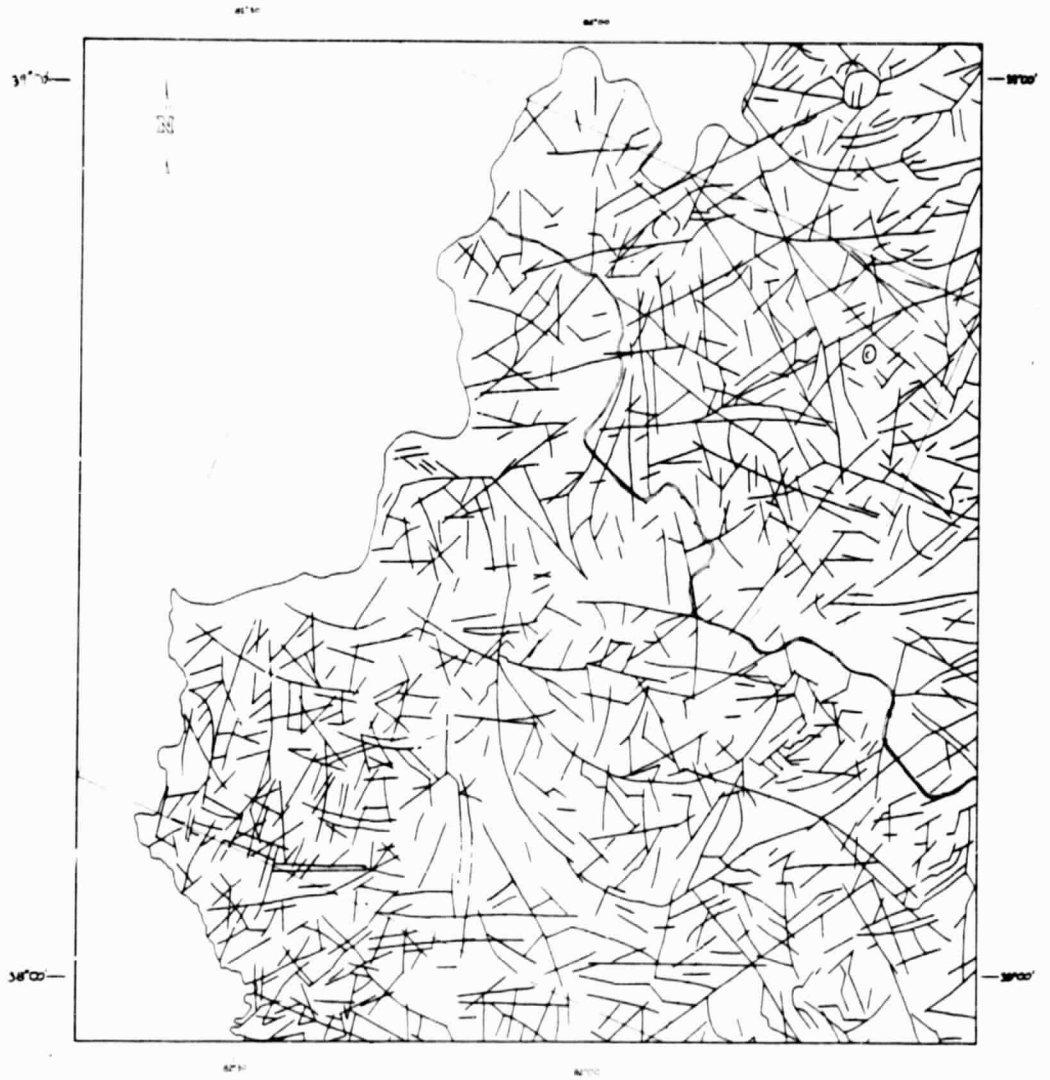

Figure 5-5. The Landsat Lineament Map of the Study Area

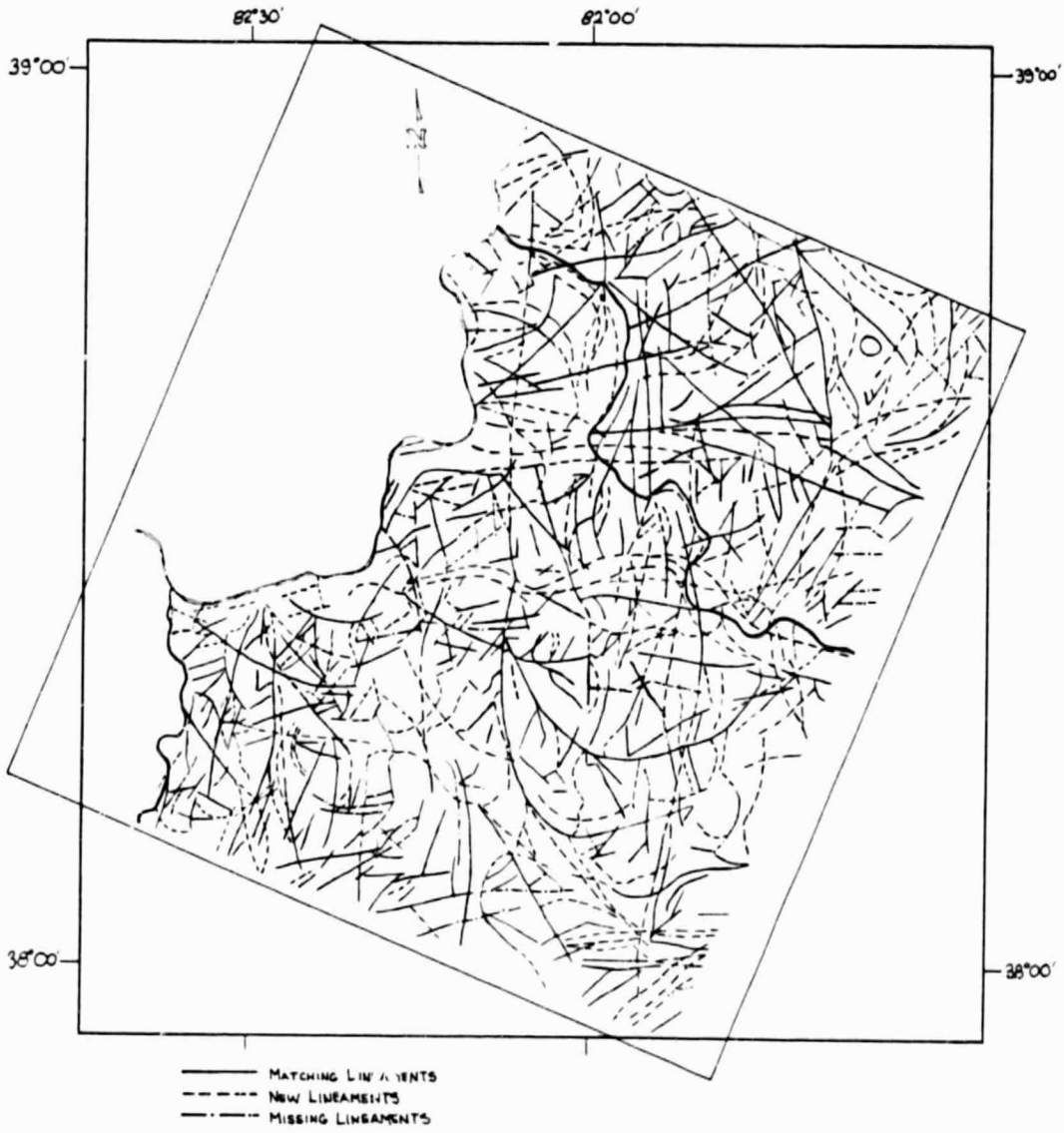

Figure 5-6. The Seasat Lineament Map of the Study Area

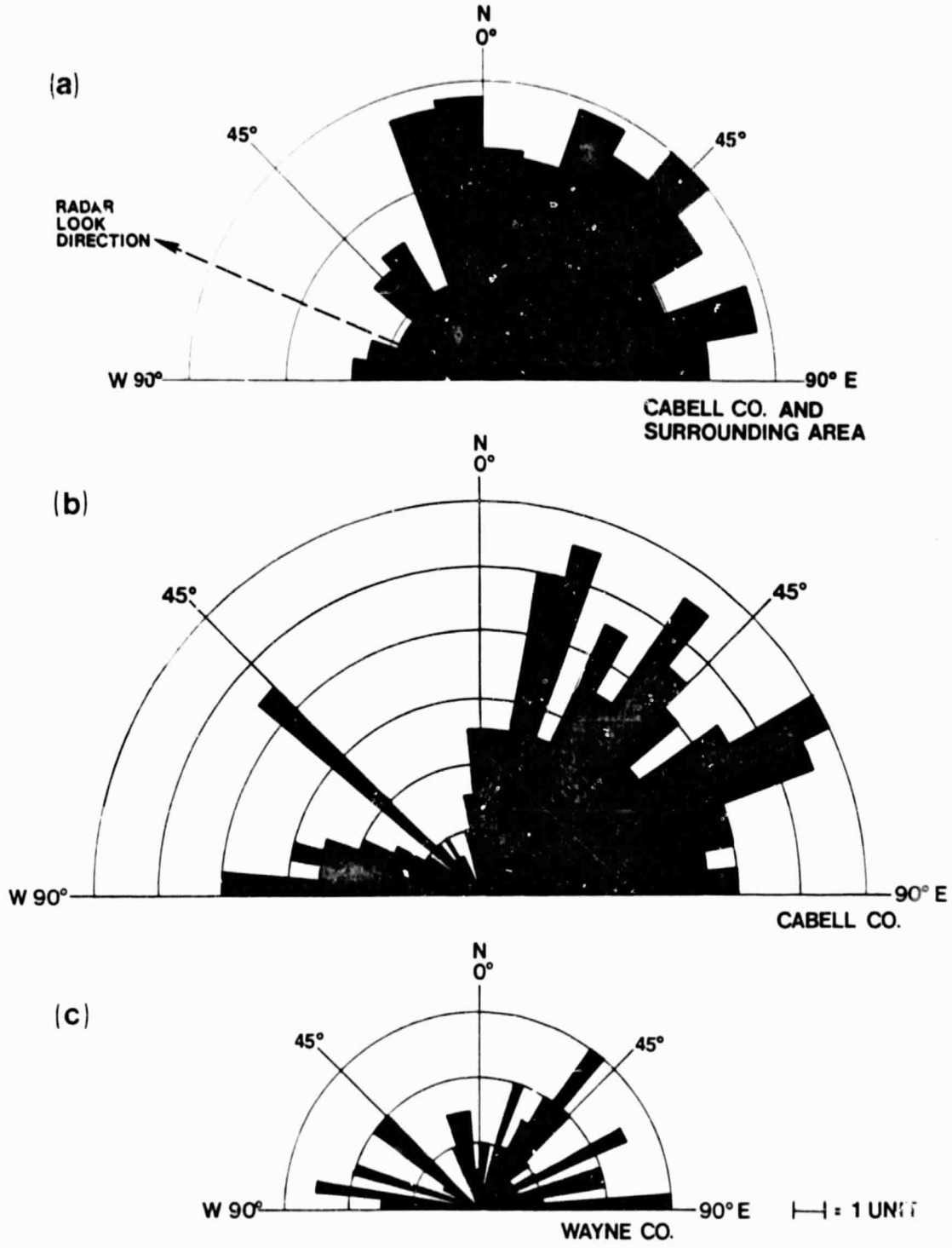

Figure 5-7. Rose Diagram for the Matching Seasat Lineaments (a) and Rose Diagrams for Cabell and Wayne Counties for the Landsat Lineaments (b and c)

parts of Wayne, Lincoln, Putnam and Mason Counties. No part lies in the states of Ohio and Kentucky. The Rose diagrams show a striking similarity inspite of the fact that the area used for the Seasat Rose diagram was larger than the one used for the Landsat Rose diagram. Rose diagrams of new and missing lineaments in the Seasat-1 SAR image are shown in Figure 5-8 as ancillary information.

5.4.1 LINEAMENT TREND ANALYSIS

When lineaments are parallel to the radar look-direction, the linears essentially disapper from the scene (Reference 38 and 3). Similarly, the radar selectively suppresses drainage features and geomorphic lineaments of low relief, whose strike direction is within 15^{o} of the direction of radar illumination (Reference 10). Sabins (Reference 38) reported that the detection of lineaments is best at approximately a right angle to the radar look angle. A comparison of lineament orientation in Figures 5-7a and 5-7b showed a reduction of lineaments in the general direction of radar look angle (67.5W), even though Figure 5-7a represents a larger area than Figure 5-7b. This reduction or an increase in missing lineaments from the Seasat lineament map is displayed in Figure 5-8b. Figure 5-5 and 5-6 show that the lineaments are, more or less, uniformly distributed over the whole area, thus one of the factors affecting the number of lineaments in a Rose diagram is the amount of area it represents. An increase in the number of lineaments in both directions making an angle of about 45 degrees to the look direction was detected. The new lineaments found in the Seasat lineament map are mostly in these two general directions (Figure 5-8a). There was no conclusive evidence for an increase in the number of lineaments in a direction perpendicular to the radar look angle. A small increase in

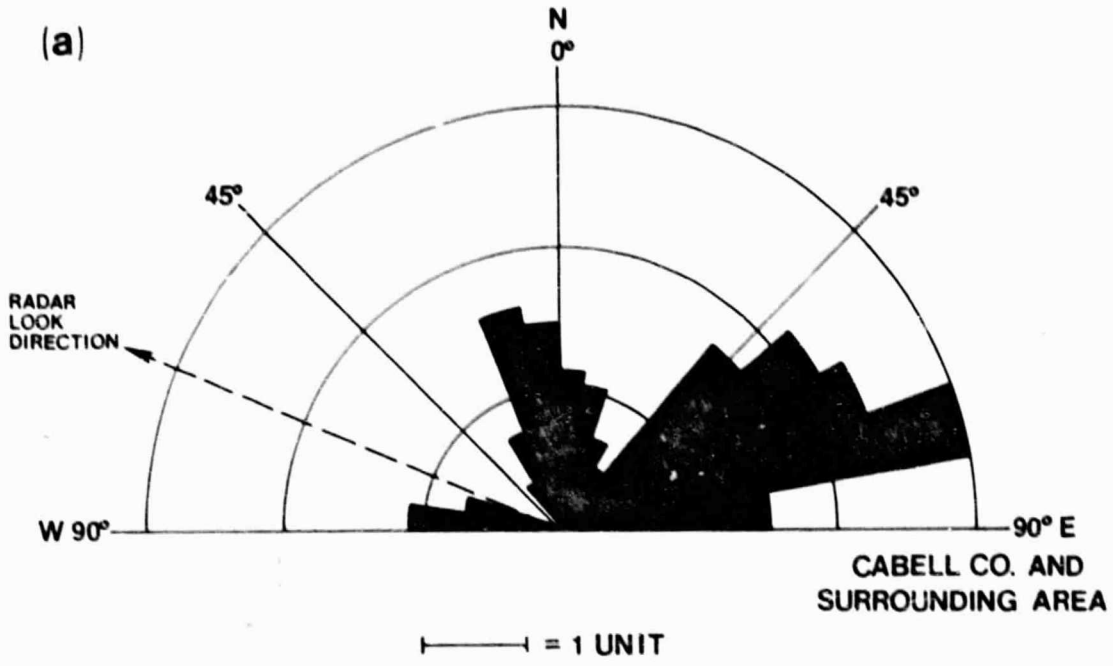

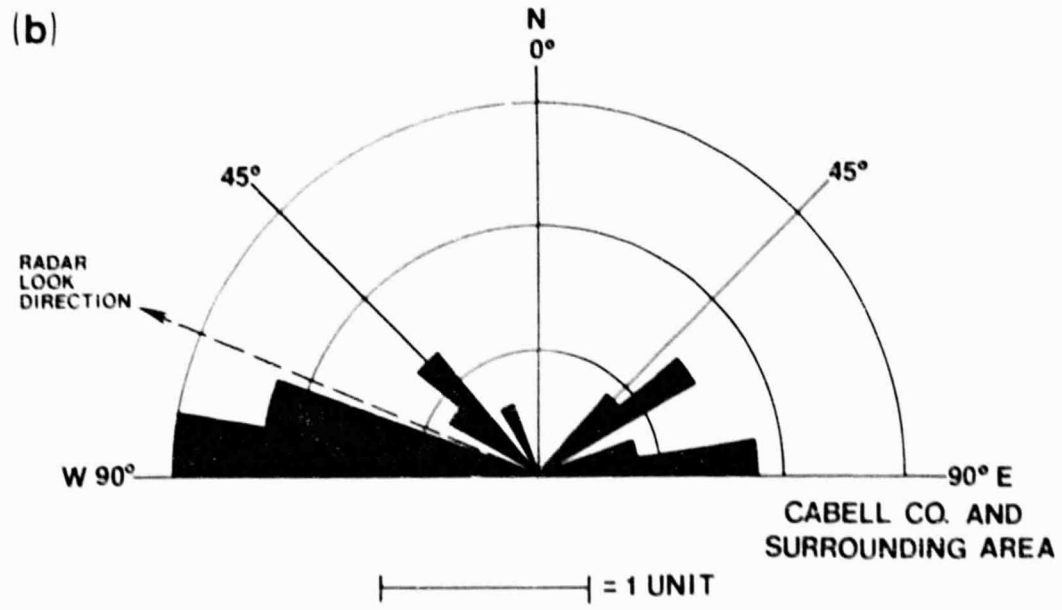

Figure 5-8. Rose Diagrams of (a) New and (b) Missing Lineaments

the number of lineaments in this direction was perhaps due to the larger area used for the Seasat lineament map.

The failure to show an expected increase in the number of lineaments in the direction perpendicular to the radar look direction may be attributed to the subtle tonal effects (required to detect lineaments) being marred by the shadows on the western slopes caused by the interactions of the N-NE trending topographic features and the nearly W-NW radar scan. The advantage of using the Seasat image over Landsat was not realized in detecting additional lineaments for the nearly N-NE direction. The increase in lineaments at about 45 degrees on both sides of the radar look direction is considered due to avoidance of supersaturation of the signal and minimization of the shadow effect mentioned above.

Selection of Seasat scene with a flight direction at about 45 degrees to the general terrain allignment would be useful. This is particularly true where the terrain causes shadows on the slopes away from the radar. The low inclination of the imaging radar beam from vertical produces layover* of all slopes that exceed about 20°. The steep slopes are excessively compressed toward the imaging direction owing to radar layover (Reference 10). The terrain in the study area, though highly variable, was small enough so as not to affect the Seasat image due to layover. Further analysis was carried out by geologists in West Virginia, results of which are discussed below.

5.5 LINEAMENT EVALUATION

Enhanced imagery of Landsat MSS (July 18, 1977), Seasat-1 SAR (August 27, 1978) and Landsat-MSS/Seasat-SAR merged

*Elevation distortions, such as the displacement of the top of a tall feature, which is closer to the radar antenna than its base and is recorded and displayed at nearer range than the base, are called layover.

data, was sent to Dr. D. Sanderson, Dr. R. Bonnett, and Professor J. Brumfield, Remote Sensing Group, Marshall University, Huntington, West Virginia for the determination of linears. The images, which had been geometrically corrected and registered to each other, covered parts of Ohio and West Virginia near Huntington, West Virginia. The images were analyzed by two groups, Bonnett and Brumfield as one team and Sanderson alone as the other team. Both groups have training and experience in image interpretation techniques and various levels of training and experience with Landsat and Seasat data. The techniques used by each group are described in the next subsection.

5.5.1 METHOD OF EVALUATION

Each group spent about two hours searching the images for linears. Sanderson (Appendixes A and B) inspected them for subtle tonal changes that were irrespective of topography. His choice of linears had to meet his own interpretation criteria. Bonnett and Brumfield (Appendix B) employed subtle tonal and textural variations and the strongly expressed joint-controlled stream patterns and topographically-expressed features as guidelines for lineament selection. Their selection involved acceptance by both members of the team. Bonnett and Brumfield picked 297 linears and Sanderson picked 93, or only one third as many, based on the more selective criteria.

The linears were drawn on acetate overlays. The orientations of the linears were measured with a goniometer and then tallied into 10 degree intervals for graphic display. Presentation of results is in the form of a Rose diagram where the length of the ray is proportional to the percentage of linears in a particular 10-degree interval. The results of their study (Appendixes A and B) are considered from three perspectives, the correlation within a group,

the correlation between the two groups, and the comparison of the results to a field study in the same area. The three persons studying the images agreed that the MSS scene was the most difficult to search for lineaments. Sanderson felt the radar and merged scenes were of the same ease in studying. Bonnett and Brumfield felt the merged scene was the easiest to work. These impressions appear to be borne out by the relative number of linears found in each scene by the two teams. It should be noted that each group first viewed the MSS scene, then the radar scene and finally the merged scene. There may be an experience factor involved; Sanderson had previous experience trying to relate roof fall problems in coal mines to linears mapped from satellite and airborne images.

5.5.2 INTRA-CONSISTENCY

Sanderson's three Rose diagrams (Appendix A) show little correspondence to one another. The MSS and merged images yielded a prominent single direction whereas the radar (SAR) scene produced a bimodal grouping. The only strong correlation among them is the NW component in the radar and merged plots. Overall, the distributions have well defined directions.

The Bonnett-Brumfield (B-B) results show a relatively good correlation among Rose diagrams. At least three or four directions appear to be common in at least two of the three images, particularly the N-S, N70 degree East and N30-40 degree West clusters. The B-B results appear to be less well defined as to strong directions. This may be due in part to the higher sample number.

5.5.3 INTER-CONSISTENCY

A comparison of the MSS Rose diagrams (Appendix A) between the two groups shows only a reasonable similarity in the N-S component. The maxima directions of each are not the same.

A similar set of Rose diagrams for the radar scenes, prepared by the two teams, yielded a closer comparison in the N-S component. Both of the directions in Sanderson's diagram appear as perhaps secondary and tertiary prominence on B-B's rose diagram. The primary direction on the B-B diagram is not found on Sanderson's results.

The flight direction of Seasat-1 radar and its westward scan (Table 4-1) highlighted the east slope of N-NE trending topographic feature. This is B-B's most prominent direction whereas in Sanderson's diagram it is virtually absent. Sanderson was perhaps aware of the potential bias the shading could have and mentally filtered this effect and with it, probably, some real linears. The peak distributions on the merged plots are at right angles to one another and in each group, the respective maxima are the strongest of the three scenes. Sanderson's secondary maxima correlates the B-B's quaternary maxima.

The radar image, out of the three scenes, yielded the best comparison between lineaments plotted by the two teams. The correlation, however, is only moderate.

5.5.4 COMPARISON TO FIELD STUDY

The results of the linear determination were compared to a joint study published by Sanderson and Duba (Reference 39) on the Huntington area. A table was prepared (see Appendix A) having the four principal joint sets identified in the field compared to the results of the Rose diagrams. The numbers in the table refer to the order of prominence of the direction on the rose diagram. A "NO" indicates the particular joint set direction didn't prominently appear on the Rose diagram. The results show that one group was not significantly better than the other in matching linears with major joint sets (if indeed there is such a correlation). One half of the twelve entries for each group resulted in

NO's, meaning that the remotely sensed data did not reveal the joint pattern very well. The radar-scan scenes gave the poorest correlation with the field data.

5.5.5 SUMMARY OF RESULTS

The amount of time required to complete lineament selection for different persons is about the same, but the number of linears selected was not proportional to time of investigation. There may or may not be an internal consistency of results of different image scans from the same area. There was only moderate correlation of results between different persons. There was only moderate correlation of lineaments with joint patterns. The results given above basically compare lineament numbers and directions with the rosettes published in an earlier work by Sanderson and Duba (Reference 39). Therefore the summary results are relatively subjective.

A comparison of MSS and radar Rose diagrams in Figure 5.7 and figures in Appendix A is given below. MSS Rose diagram 5.7 was reproduced from Reference 25 and the radar Rose diagram was prepared by the author. Rose diagrams for both MSS and radar in Appendix A were prepared by Bonnett-Brumfield (B-8) and Sanderson. The MSS Rose diagrams were quite similar except that Sanderson had generally fewer lineaments selected. Sanderson showed a strong NE trend, which is nearly the general trend of the topographic features in the area. Perhaps he mentally filtered all the other lineaments in the NE quadrant. The general trends on the radar Rose diagrams were similar. Both B-B and Sanderson detected fewer lineaments in general and Sanderson detected almost none in the NNE section. Perhaps they recognized more lineaments in the NNW direction at the expense of those in the NNE section. Lineaments in the NNW direction match quite well in all the three cases. Further

studies might include length-stroke orientation analysis, geographic location of lineaments and reproducibility of the lineament study.

SECTION 6 - LAND COVER CLASSIFICATION

The application of Seasat-1 SAR imagery to landcover classification was examined. Classification based on density slicing was not possible due to the shadows on the western slopes and signal saturation on the eastern slopes. Direct classification from Seasat SAR data was not considered due to its having only one polarization (HH). Its usefulness for digital landcover classification mapping was explored by considering it as an additional multispectral channel. Two Landsat scenes, one from July 18, 1977 and the other from May 11, 1978 were selected for classification and to study the effects of adding the Seasat SAR channel to the Landsat channels. A ratio image was added as described in Section 5.4. Both the Landsat and Landsat/Seasat merged images were used for classification, so that the effect of adding the Seasat SAR channel could be studied. The May 11 image was classified as an additional information base.

All three registered data sets (May 11, 1978 Landsat, July 18, 1977 Landsat, and the July 18 1977 Landsat merged with August 27, 1978 Seasat) were used for landcover classification.

6.1 CLASSIFICATION PROCEDURES

The classification procedure (Figure 6-1) essentially includes signature development, signature review and signature utilization for classification. Signature development can either be supervised or unsupervised. Training sites containing distinct spectral properties were not very well defined; therefore unsupervised classification was used in all three cases. The training site mentioned in Figure 6-1 consisted of one or more small subsections which were fairly representive of the whole area rather than specific areas

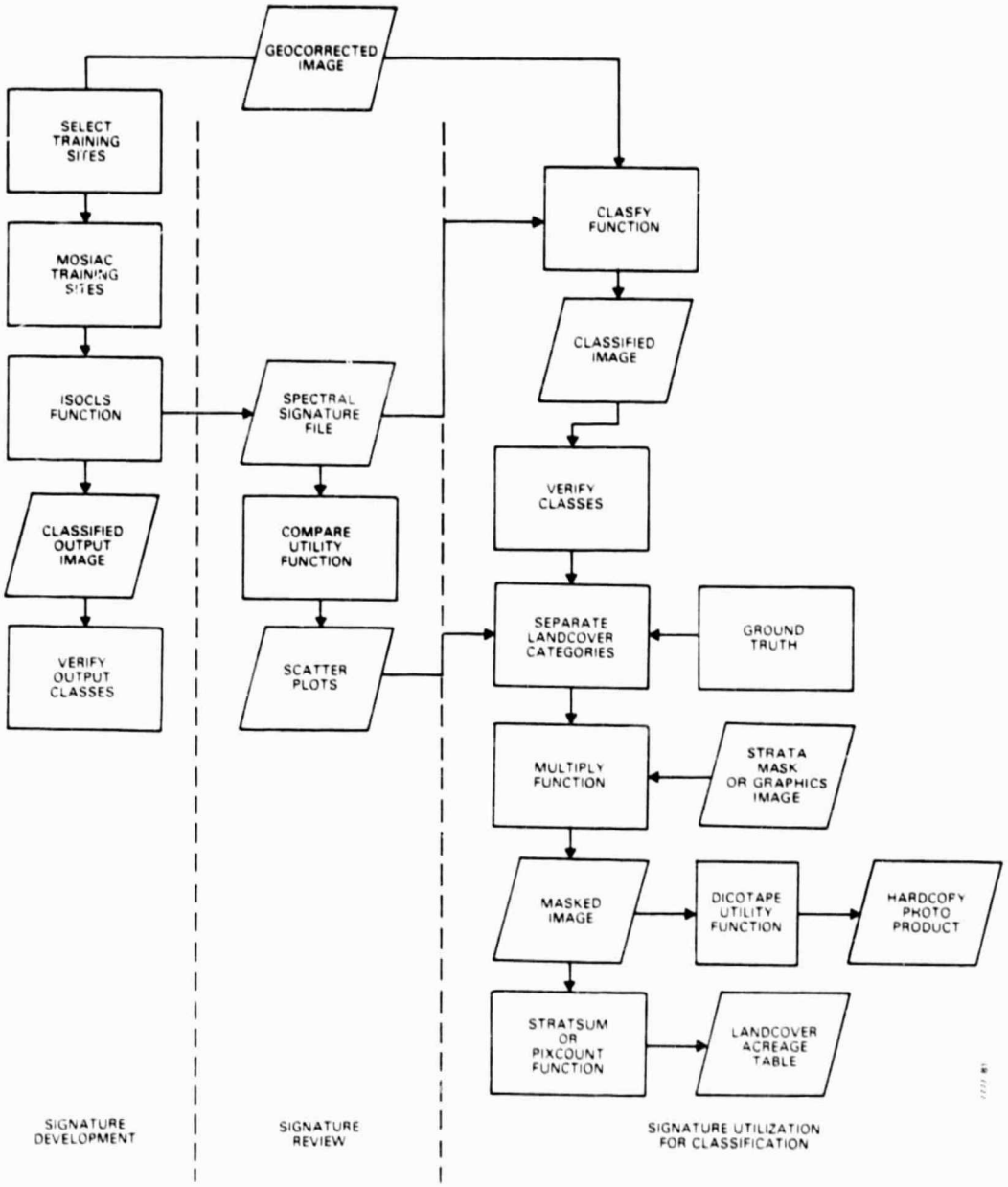

Figure 6-1. Functional Diagram for Land Cover Classification

with distinct spectral properties. If there is more than one subsection, they are merged and then used as input into the ISOCLS function. ISOCLS uses a clustering algorithm to partition a given set of multivariate data points, with little or no knowledge about the actual distribution of the data, into disjoint sets of similar data points. This function generates spectral signatures for a specified number of groups or classes and produces a classified image of the input training site image. The output image was verified either by displaying the image or by getting a histogram of the pixel frequencies. The statistical file listing was examined and also input into the COMPARE utility function which produced scatter plots for any two specified bands. The most useful scatter plots were between bands 5 and 7. One such plot for May 11 is shown in Figure 6-2. The center of the circle (or ellipse) represents the average reflectance for the two bands and the spread in reflectance in each class is given by the circle diameter (or ellipse axis). These scatter plots, along with ground truth information, help in separating the spectral classes into the landcover categories.

After the statistics were developed and reviewed, they were used to classify the whole image; subsets of the image were previously used to develop the preliminary signatures. This was done using the function CLASFY, which classifies a multiband input image into spectral types according to spectral statistics by using a maximum likelihood decision rule. The output classes were then separated for different landcover categories using the ground truth information available and the scatter plots. The landcover image thus produced was then multiplied by the strata mask image, which generated a masked image containing only the Cabell County area. This was input into the PIXCOUNT function which produced the landcover statistics which were later converted into acreage.

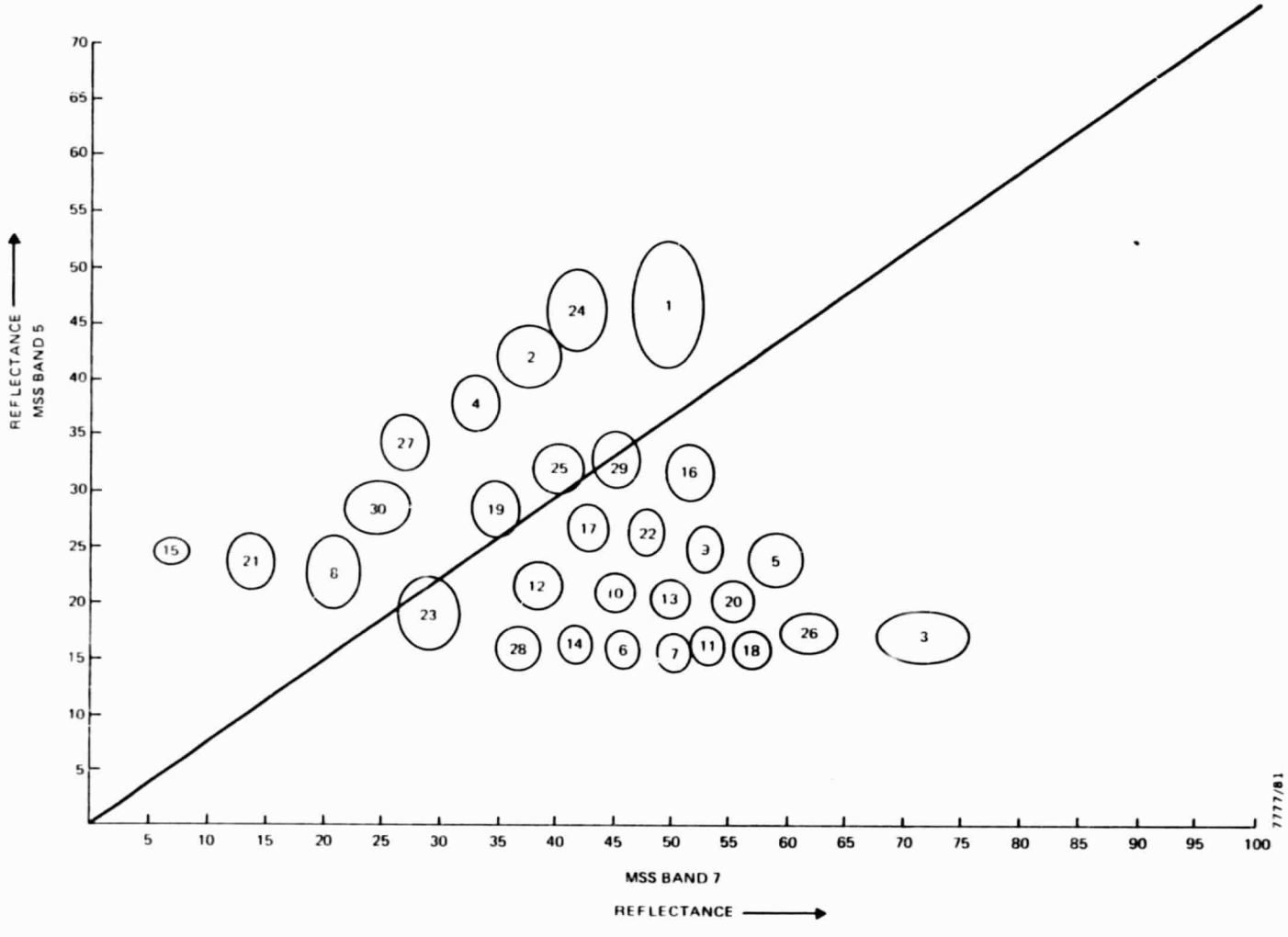

Figure 6-2. Scatter Plot of Statistical Class Averages Between MSS Bands 5 and and 7. Standard Deviations are Indicated by Circles or Ellipses

The July 18, 1977 and MSS/SAR merged classified images for Cabell County are shown in Figures 6-3 and 6-4 respectively. A comparison of landcover areas for various landcover categories from different data sources is shown in Table 6-1. The May 11, 1978 (rural classification) had an additional signature for rural areas. The data source for the West Virginia Geological and Economic Survey (Reference 51) was the color-infrared aerial photography for 1973.

6.2 CLASSIFICATION EVALUATION

Classified images for July 18, 1977 and MSS/SAR merged image were sent to participating geologists in West Virginia and Kentucky. They were Mr. C. Roueche at the Kentucky-Ohio-West Virginia (KYOVA) Interstate Planning Commission, Professor J. Brumfield of the Marshall University, Dr. P. Lessing of the West Virginia Geological and Economic Survey, and Dr. W. Adams of the Eastern Kentucky University. Roueche and Brumfield worked as a team and they had access to the May 11, 1978 classified image. The statistical information, listed in Table 6-1 were sent along with the classified images.

The evaluation of the classification results received from them as a private communication are presented below (see Appendix C, D and E for communications). The authors' own evaluation is presented here. The methods of analyses were significantly different in each case, but the conclusions arrived at are similar. The methods of evaluation are presented in the next subsection. The results are presented separately for Landsat MSS and MSS/SAR merged data in the second and third subsections, and the comparison of Landsat MSS and MSS/SAR merged are given in the fourth subsection.

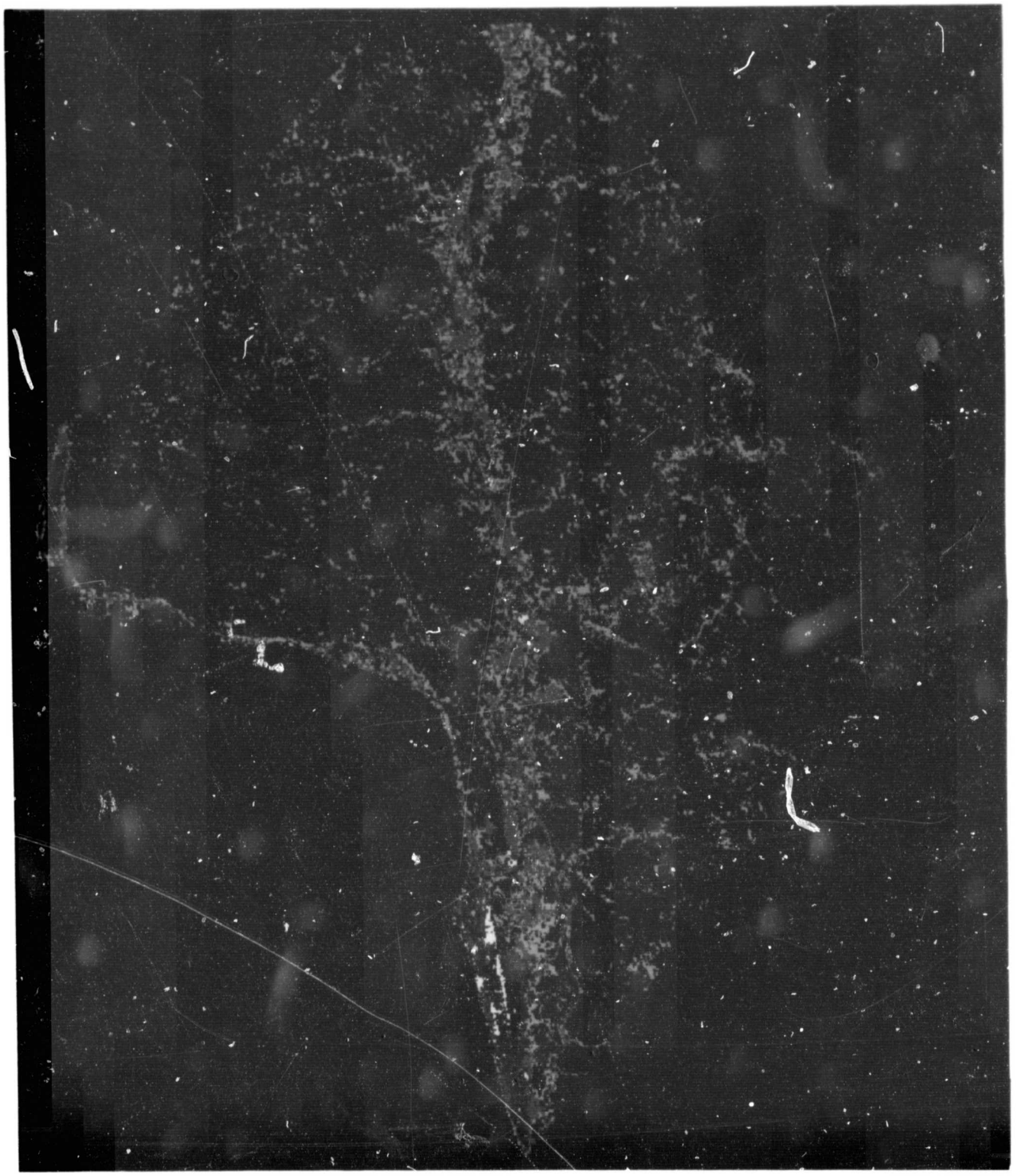

The color assignments are as follows: High-density residential in dark grey; medium-density residential in orange; low-density residential/rural in sand; commercial in red; industrial in white; water in dark blue; mixed pixels in black; agricultural and fields in olive; and forests in dark green.

Figure 6-3. The July 18, 1977 Landsat Classified Image for Cabell County

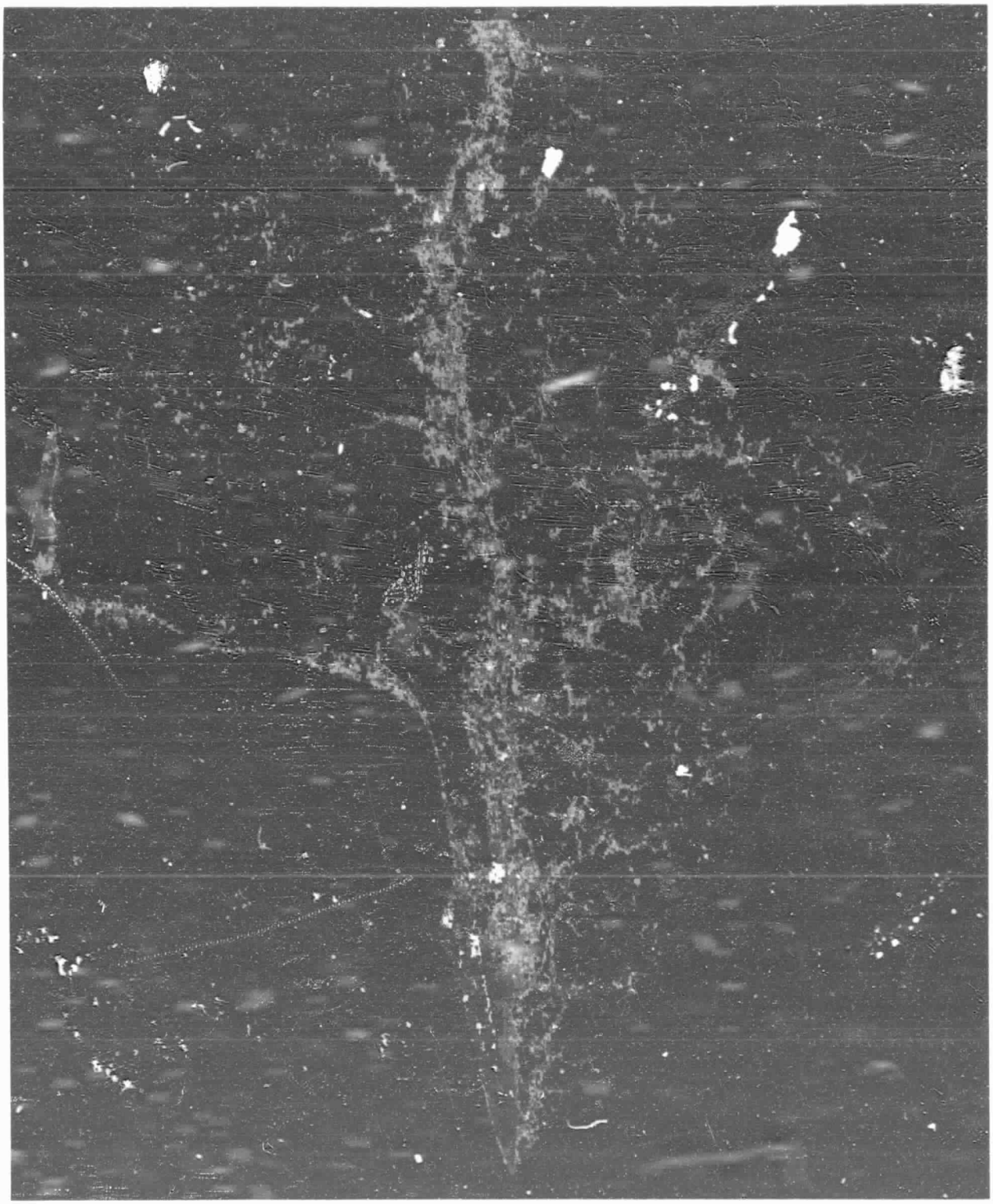

The color assignments are as follows: High-density residential in dark grey; medium-density residential in orange; low-density residential/rural in sand; commercial in red; industrial in white; water in dark blue; mixed pixels in black; agricultural and fields in olive and forests in dark green.

Figure 6-4. The Merged Landsat-MSS/Seasat-SAR Classified Image for Cabell County

Table 6-1. Comparison of Land Cover Areas for Different Land Cover Categories From Different Data Sources

LANDCOVER CATEGORY	WEST VIRGINIA GEOLOGICAL AND ECONOMIC SURVEY (WVGES)	MAY 11, 1978 LANDSAT DATA		JULY 18, 1977 LANDSAT DATA		LANDSAT-MSS/SEASAT-SAR MERGED DATA	
	ACRES	ACRES	PERCENT OF WVGES	ACRES	PERCENT OF WVGES	ACRES	PERCENT OF WVGES
URBAN OR BUILT-UP LAND							
HIGH DENSITY	11,515	2,709	94.5	3,051	93.6	2,532	96.4
MEDIUM DENSITY		8,172		7,729		8,573	
COMMERCIAL	2,076	924	44.5	757	36.5	1,221	58.8
INDUSTRIAL	1,631	317	19.4	532	32.6	624	38.3
SUBTOTAL	15,222	12,122	79.6	12,069	79.3	12,950	85.1
AGRICULTURAL LAND	16,932	13,386	79.1	13,241	78.2	11,319	66.8
LOW DENSITY RESIDENTIAL OR RURAL	–	18,015	–	18,590	–	17,620	–
FOREST AND WETLAND	146,909	134,305	91.4	133,942	91.2	136,122	92.7
WATER							
WATER	3,539	2,774	–	2,660	–	2,917	–
MIXED	0	772	–	872	–	445	–
SUBTOTAL	3,539	3,546	100.2	3,532	99.8	3,362	92.7
GRAND TOTAL	182,602	181,374	99.3	181,374	99.3	181,373	99.3

7777/81

6.2.1 METHODS OF EVALUATION

Roueche and Brumfield (Appendix C) evaluated one set of classification maps. They selected several verification sites of each landcover category from selected regions of Cabell County. The classification was verified using black and white aerial photography of April 1976 and April 1980 at a scale of 1:24,000. The photography was furnished by the U. S. Army Corps of Engineers, Huntington District, Huntington, WV to the KYOVA Interstate Planning Commission. Two evaluation methods for land category accuracy were used. (1) Determination of selected spatial representation for landcover categories of the classified images, and (2) acreage statistics of the classified categories.

For accuracy assessment, each set of land category statistics were compared to a 1968 comprehensive land-use planning study for the SMSA area. The study included Cabell County and more projections through 1990 for acreage land use. The relative accuracies of the Landsat MSS classified and merged MSS/SAR classified images were compared using the spatial representation of the landcover classification and overall category acreage estimates.

Lessing (Appendix D) compared the acreage estimates from the MSS/SAR classifications with acreage calculated from color infrared photography, topographic maps, and West Virginia Geological and Economics Survey land use maps.

Adams (Appendix E) used sampling of selected identical areas of MSS and merged MSS/SAR classified images to note changes in classification. A comparison was then made of the landcover shown on the images with that shown on other imagery and maps. To aid in the comparison of the two 1:250,000 scale images, a grid overlay divided into one-half square inch units were attached in an identical fashion to each image. The images were then placed on a Bauch and Lomb

Zoom Transfer Scope model ZT4, so that the MSS/SAR image was projected onto the MSS image. Illumination was adjusted to full intensity using front and backlighting for the merged MSS/SAR image. By rapidly manipulating the rheostat switch to alternately increase and decrease light intensity on the MSS image, the areas that were classified differently could be readily identified. Selected areas were examined in various parts of Cabell County.

The author used the West Virginia Geological and Economic Survey (WVGES) data (Reference 51) for accuracy assessment. All the calculations are in acres and the percentage calculations used in the text represent the percentage of the WVGES values.

The acreage statistics are shown in Table 6-1.

6.2.2 LANDSAT CLASSIFICATION RESULTS

Roueche and Brumfield (Appendix C) found the overall spatial landcover categories relative to land-use categories generally quite good. Several categories, for example commercial, industrial, and high-density residential, depicted the areas quite well in terms of existing land usage when compared to their interpretation of the 1976 and 1980 aerial photography and their knowledge of the area. The estimated locational representation for these three landcover/use categories appears approximately 80 to 85 percent accurate. Low- and medium-density residential categories appear to depict the land usage pattern well. However, road patterns are often confused with those categories. Consequently, aerial extent of low-density residential is apparently overstated. The agricultural category seems to be understated and is probably confused with low-density residential areas.

The water category depicts the Ohio River whereas the Guyandotte River and several 3 to 8 acre ponds and treatment

facilities are not evident. A portion of the mixed/ unclassified category appears to be the Guyandotte River. The forest category was not evaluated due to lack of time. Because of small scale and perhaps no detectable change in the area, no significant difference in categories could be determined between 1977 and 1978 Landsat MSS classified images by visual inspection.

Lessing (Appendix D) found that the major differences were a lower estimate for forest acreage and higher estimate for urban acreage for the Landsat classification. He believes that low-density residential is the source of this error. If the low-density residential was changed to agriculture and forest, the acreage would be in better agreement.

Adams (Appendix E) did not make a direct evaluation of the Landsat classified image. He made a comparative study of the two classifications.

An observation by the author is worth mentioning before the classification evaluation is presented. The low-density residential/rural category perhaps constitutes three elements: (1) A small portion of housing and other man-made structures along county roads in the valleys; (2) a relatively larger portion of lawns, vacant lots and other areas along the roads, and (3) a major portion of relatively thinned forests, surrounding these housing corridors. A division of this category into urban, agricultural and forest categories based on judgmental estimates will be used to account for better estimates for these three categories.

The results of the author's analysis of the landcover classification are presented below. The accuracy calculations are based on the West Virginia Geological and Economic Survey (WVGES) (Reference 51). WVGES's 15 original landcover subclasses were grouped together according to similar landcover, such as residential with mixed and other urban or

built-up land, reducing landcover categories to 8, which corresponded to the Landsat landcover categories. WVGES had no corresponding category to the Landsat low-density residential category. The corresponding categories were compared and percentages of Landsat categories to WVGES categories were computed. These grouping and the accuracy calculations are tabulated in Table 6-1. About 80 percent of the urban or built-up category was correctly classified. This includes the city of Huntington and the new development corridor along highways 60 and 64. The remainder of the built-up land is included in the low-density residential category. About 94 percent of the high- and medium-density residential in the urban or built-up category was correctly classified. The commercial and industrial subcategories had 37 to 45 and 19 to 33 percent accuracy in the two Landsat classifications. The shortfall in the last two subcategories may be due to miss-classification of parking lots, decorative landscaping and bare ground surrounding commercial and industrial building as high- and medium-density residential. This may be due to spatial non-separation of these areas from the surrounding residential areas. About 80 percent of the agricultural land was correctly classified and the remaining 20 percent of this category was classified as low-density residential for the reasons mentioned above. About 91 percent of the forest category is correctly classified while the remaining 9 percent was classified as low-density residential. The water category was nearly 100 percent accurate for the larger water bodies. The mixed pixel subcategory has been included in the water category because the mixed pixels are partially water pixels along the Ohio and Guyandotte rivers. All the above calculations are for landcover estimation accuracy and not related to spatial accuracies.

6.2.3 LANDSAT-MSS/SEASAT-SAR MERGED IMAGE CLASSIFICATION RESULTS

Roueche-Brumfield (Appendix C) found the overall spatial representation of landcover categories relative to general land use categories quite good and similar to Landsat classification except for the improvements over Landsat as stated below. The estimated locational accuracy appears to approach 90 percent. The water category did depict one sewage treatment pond, though other ponds were not present. The Guyandotte river was classified as mixed pixels.

Lessing (Appendix D) had no comments about the merged classification other than a comparison between Landsat and merged classifications.

W. Adams (Appendix E) subdivided the classified images (1:250,000 scale) into one-half inch subsections which showed that the classification of the merged image generally caused a shift from a higher order of land use/cover to a lower order of land use/cover. Seventy-four percent of the classification changes in the areas examined were of this type. The most frequently occurring change was from low-density residential to agricultural land uses. This was closely followed by the change of low-density residential to forest, and by medium-density residential to low-density residential. Portions of images covering urban areas often showed more commercial and industrial areas on the merged image.

The author's analysis of the merged image classification showed an improvement over Landsat image classification. The accuracies of urban or built-up land was estimated at about 85 percent. About 96 percent of the high and medium-density residential portion of the above category was correctly classified, whereas, the commercial and industrial/transportation portions were only 59 and 38 percent accurate

respectively. The agricultural category had an accuracy of 67 percent and the forest category was 93 percent accurate. The water category was about 95 percent correctly classified. Accuracy for the low-density residential category was not assessed because it represents the combined residential, agricultural and forest categories as explained earlier.

6.2.4 LANDSAT MSS AND MERGED LANDSAT-MSS/SEASAT-SAR CLASSIFICATION COMPARISON

Roueche-Brumfield (Appendix C) considered low-density residential as urban and built-up land, which is not entirely correct, and thus they concluded that the low- and medium-density residential acreage estimate is optimistic by approximately 500 percent when compared with existing figures from the comprehensive study (Reference 24). However, they found that the merged data classification categories for high- and medium-density residential depict the overall location quite well in terms of land usage patterns, whereas the Landsat MSS classification tends to over emphasize medium-density residential land usage patterns. Agricultural and low-density residential categories appear to be confused on both Landsat and merged classified images.

Also, there is confusion on both classified images of road patterns with medium- and low-density residential. Additionally, smaller rivers and ponds tend to be mis-classified except for one large waste-treatment pond which was correctly identified on merged classification. Commercial, industrial, and high-density residential areas were all identified with reasonable accuracy in terms of existing land-use pattern. The merged classified image appears to depict and locate these categories more accurately when compared to their interpretation of the aerial photography and their knowledge of the area. It seems that the merged Landsat-MSS/Seasat-SAR classified image would be the most suitable for regional planning activities. However, the

confusion of roads with medium- and low-density residential and low-density residential with agricultural patterns would suggest their utility for only very generalized planning.

Adams (Appendix E) arrived at a tentative conclusion that the merged classification appears to present a more accurate distribution of landcover. He further concluded that the distribution and categorization of landcover from the merged data appear to be more correct than a single Landsat scene. The Landsat/Seasat merged classification was affected by the corner-reflector phenomena associated with look direction and street direction. When the street orientation is parallel to the satellite (Seasat) path, the radar beam is reflected back towards the antenna from the corner reflectors formed by the street and the buildings. This produced some spatial misclassification of the commercial/industrial categories, but the effect was not very pronounced except in the middle of Guyan Estates industrial park on the east side of Huntington.

An improvement in accuracy in classifying man-made structures was reported by Wu (Reference 54) by using Landsat/Seasat merged data; however he also reported improved forest species separation for forest cover. This type of analysis (forest species separation) was not attempted by the author due to time constraints. Wu elected a test area with very slight surface slope variation and with landcover types relatively free of a heavy concentration of commercial buildings, both of which were present in the area analyzed by the author. In spite of these drawbacks, an improvement in discriminating man-made classes was detected in the author's study. Further study concerning the use of merged data set to improve landcover classification and area estimation is warranted. Clark (Reference 7) reported significant improvements in the land-use classification accuracy in urban setting, such as industrial, commercial

and services, communications and utilities by using the Landsat/Seasat merged imagery.

The Landsat (July 18, 1977) classification statistics were compared with Landsat (July 18, 1977)/Seasat(August 27, 1978) merged classification statistics. In the Landsat/ Seasat merged image, the additional Seasat SAR information helped to reclassify some of the pixels into a different landcover category. The merged classification was better in acreage and spatial estimation accuracy, therefore it is fair to assume that the reclassification resulted in a more accurate classification.

The impact of reclassification can be assessed from a contingency table for these two classifications (Table 6-2). A contingency table gives a pixel by pixel comparison of each landcover category in one classification with each landcover category in the other. If there are i categories in one classification and j categories in the other, a matrix M of i rows and j columns can be produced using IDIMS function CONTABLE (Reference 9). Such a matrix is shown in Table 6-2 for July 18, 1977 Landsat and Landsat/Seasat merged image classifications. Pixels which are classified to the same landcover category are on the diagonal (from left top to bottom right), and pixels which are classified differ- ently lie off this diagonal. The element (i, j) of the matrix M indicates that a portion of the ith category of one classification was reclassified as a portion of the jth category of the other classification. Similarly the fractional value in the element (i, j) of the matrix is the ratio of the number of pixels in that element to the sum of all the pixels in the ith row (sum of these fractional values along

Table 6-2. Contingency Table Showing Pixel by Pixel Comparison of Each Landcover Category in the Landsat and Landsat/Seasat Merged Classifications.

LANDSAT (JULY 18, 1977)/ SEATSAT (AUGUST 27, 1978) MERGED CLASSIFICATION	JULY 18, 1977 LANDSAT CLASSIFICATION									
	HIGH DENSITY RESIDENTIAL	MEDIUM DENSITY RESIDENTIAL	LOW DENSITY RESIDENTIAL	COMMERCIAL	INDUSTRIAL	MIXED	WATER	AGRICULTURAL	FOREST	TOTAL PIXELS
HIGH DENSITY RESIDENTIAL	2750	615		406	320	7				4098
	0.67	0.15		0.10	0.08	0.00				1.00
MEDIUM DENSITY RESIDENTIAL	1677	5526	5756			179			739	13877
	0.12	0.41	0.41			0.01			0.05	1.00
LOW DENSITY RESIDENTIAL	62	5003	12344			132		1677	9304	28522
	0.00	0.18	0.43			0.00		0.06	0.33	1.00
COMMERCIAL	268	957		752						1977
	0.14	0.48		0.38						1.00
INDUSTRIAL	154	410	5	67	360	13	1			1010
	0.15	0.41	0.00	0.07	0.36	0.01	0.00			1.00
MIXED	28				146	544	3			721
	0.04				0.20	0.76	0.00			1.00
WATER					35	385	4301			4721
					0.01	0.08	0.91			1.00
AGRICULTURAL			260					12315	5749	18324
			0.01					0.68	0.31	1.00
FOREST			1731			37		7442	201136	220346
			0.05			0.00		0.03	0.92	1.00

NOTE: THE WHOLE NUMBERS REFER TO PIXELS COMMON TO THE LANDCOVER CATAGORIES REPRESENTED BY COLUMN AND ROW FOR THE TWO CLASSIFICATIONS. THE FRACTIONAL NUMBERS REPRESENT THESE PIXELS AS A FRACTION OF THE LANDCOVER CATEGORY IN THE MERGED CLASSIFICATION. SEE TEXT FOR DETAILS.

the row is 1.00). The fractional values indicate the percentage of pixels in the merged classification which came from different categories of the Landsat classification. For example, the high-density residential category of the merged classification consists of the following percentages of the various landcover categories of July 18, 1977 classification:

67 percent of high-density residential
15 percent of the medium-density residential
10 percent of the commercial and
8 percent of the industrial

categories. Normally, if the relative accuracy of the two classifications is unknown, the above results would be interpreted as 15 percent confusion between the medium-density residential of the merged classification and high-density residential of the July 18, 1977 Landsat classification, and so on. But we know from the previous discussion that the merged classification was more accurate than the Landsat classification, therefore, Table 6-2 represents reclassification of Landsat classification into more accurate classification. However, for further discussion we will consider Table 6-2 as a Confusion Table. Values along the diagonal will be considered a measure of accuracy, since these represent the same landcover category in both the classifications, and values off the diagonal will be considered a measure of confusion between Landsat and Landsat/Seasat merged categories. In the following discussion the adjectives

"Mainly" refers to values of more than 20 percent
"Moderately" refers to values between 10 and 20 percent, and "Marginally" refers to values of less than 10 percent.

About 67 percent of the high-density residential was correctly classified and was moderately confused with the medium-density residential and commercial categories and marginally with the industrial category. About 41 percent pixels in the medium-density residential were correctly classified and were mainly confused with the low-density residential, moderately with the high-density residential and marginally with the mixed categories. The low-density residential was about 43 percent correctly classified and was mainly confused with the forest category, moderately with the medium-density residential and marginally with the agricultural category. The commercial and industrial categories were about 37 percent accurate and were mainly confused with the medium-density residentials with moderate confusion with the high-density residential. The industrial category was also marginaly confused with the commercial and mixed categories. All the man-made categories were confused mostly with each other with the exception of low- and medium-density residential, which were also confused with the agricultural and forest categories. The confusion between man-made categories was due to a small reflectance transition between these categories and due to the existance of spatial inseparability of these categories.

The mixed category, which was mostly water/land mixed pixels, was mainly confused with the industrial category and marginally with the high-density residential. The water category was generally correctly classified (91 percent) and was marginally confused with the mixed category which was mostly water. The agricultural category was about 68 percent accurate and the main confusion was with the forest category. About 92 percent of the forest category was correctly classified with marginal confusion with the agricultural and low-density residential categories. The overall accuracy given by the ratio ND/NT was about 82 percent,

where ND is the total number of pixels along matrix diagonal and NT is the total number of pixels classified.

SECTION 7 - SUMMARY AND CONCLUSIONS

The Seasat-1 SAR data set was used to map lineaments in the selected test area. The Landsat and Landsat/Seasat merged data sets were used as supplementary information. The mapped Seasat SAR lineaments and Rose diagram were compared with the corresponding Landsat lineaments and Rose diagram. The lineaments and the Rose diagrams from the two sources matched quite well. Werner (Reference 48) reported only 13 percent coincidence between any two sources of photo-lineaments. The significantly better match (80 percent) between Landsat and Seasat lineaments in this case is attributed to the terrain involved and to the supplementary information base used in the processing.

About 6 percent of the Landsat MSS lineaments were missing from Seasat SAR lineament map. The missing lineaments were either small, or parts of other lineaments and existed in places of doubtful surface structure. No major lineament was found to be missing. About 20 percent (based on number of straight lineaments) new lineaments were found in the study area resulting in a net gain of 14 percent additional lineaments on the map. These estimates were based on the number of straight lineaments only. The new lineaments were found to be either extensions of matching lineaments or totally new, significant lineaments.

An increase in the number of lineaments detected at about 45 degrees on both sides of the radar look direction was observed. Similarly, a decrease in the number of lineaments in a direction parallel to the radar look direction was observed. The increase in the number of lineaments in a direction perpendicular to the radar look direction was attributed to the larger area used for the Seasat lineament map than for the Landsat lineament map.

No direct verification of the new lineaments was possible but the extent of matching lineaments lends confidence in the existence of new lineaments. Therefore the value of Seasat-1 SAR data for the enhancement and detection of lineaments is demonstrated. It should be preferred to Landsat wherever it is available and only one image is interpreted. The Landsat/Seasat merged data is better still. The information content is increased and complemented in the merged image as compared to the Landsat and Seasat images alone. The color composite described in this document has the additional advantage of bringing out the surface structure visually, emphasizing the lineaments, and displaying "tonal" lineaments.

Photointerpretation and mapping of lineaments from the remotely sensed data were greatly facilitated by computer manipulation of digital values to produce enhanced imagery. Seasat SAR and Landsat MSS images can best be enhanced for lineament plotting by using a simple contrast stretch procedure, which expands the original range of digital values to the full range of the image display device/medium. A number of other enhancement methods, such as box filters, principal components, and edge enhancement were judged inferior to this method by other investigators (Reference 32).

An improvement in the landcover classification in acreage and spatial accuracy was demonstrated by using the Landsat-MSS/Seasat-SAR merged data. In particular, an improvement in the classification accuracy in the residential/build-up and forest categories was noticed. However, a slight reduction in accuracy in the agricultural and water category estimation was found.

In recent years, there has been a trend to drastically slash funds for regional planning. A landcover classification using remotely sensed imagery can be a cost-effective way for planners to monitor land-use in the future. Therefore, achieving increased classification accuracies using merged data from different sensors is important. The merged data classification map sent to West Virginia for field verification lead one planner to comment, "I was extremely impressed with the overall accuracy of the map and would be interested in integrating this type of land-use data into our planning program. An annual or bi-annual update would be very useful in plotting the growth changes over a given time span," (Private Communication).

The low-density residential category posed some problems. The differences in the classification procedure used by planning agencies and the one used here to classify the low-residential category was the main reason for the confusion in interpreting this category. The planning procedure used by the various planning organizations such as Metropolitan Planning Organizations (MPOs) etc., sub-divides this category into residential, agricultural and forest land based on criteria which are impossible to implement in this classification due to limitations of the MSS data. The spatial accuracy was found to be very good in the field verification as discussed in subsection 6.2.2.

APPENDIX A

Summary of Results of Linear Determination
Dewey D. Sanderson

Introduction

Three high altitude, remotely sensed image scans were studied for their linear content. The three scans included Landsat-MSS, Seasat-Radar and a composite or merged scan of the previous two. The area of Huntington, W. Va. is included in the scenes.

The images were analyzed by two groups Richard Bonnett and James Brumfield as a team and Dewey Sanderson by himself. Each group spent about two hours searching the images for linears. Sanderson inspected for subtle tonal changes that were irrespective of topography. His choice of a linear had to meet his own mental template. Bonnett and Brumfield selected both subtle lineations and the strong ones topographically expressed. Their selection involved acceptance by two people. Bonnett and Brumfield picked 297 linears and Sanderson picked 93, or only one third as many.

The linears were drawn on acetate overlays. The orientations of the linears were measured with a goniometer and then tallied into 10^{o} intervals for graphic display. Presentation of results is in ray diagram form where the length of the ray is proportional to the percentage of linears in a particular 10^{o} interval.

The result of the short study are considered from three perspectives, the correlation within a group, the correlation between the two groups and finally the comparison of the results to a field study in the same area.

The three persons studying the images agreed that the MSS scene was the most difficult to search. Sanderson felt the radar and merged scenes were of the same ease in studying. Bonnett and Brumfield felt the merged scene was the easiest to work. These impressions appear to be born out by the relative number of linears

found in each scene. It should be noted that each group first viewed the MSS scene, then the radar scene and finally the merged scene. There may be an experience factor aquired. Sanderson has had previous experience a few years ago trying to relate roof fall problems in coal mines to a coincidence of linears mapped from satelite and airborne images.

Intra-consistency

The results of Sanderson's three ray diagrams show little correspondence to one another. The MSS and merged images yielded a prominent single direction whereas the radar scene produced a bimodal grouping. The only strong correlation among them is the NW component in the radar and merged plots. Overall, the distributions have well defined directions.

The Bonnett-Brumfield (B-B) results show a relatively good correlation to one another. At least three or four directions appear to be common in at least two of the three, particularly the N-S, N70^{o}E and N30-40^{o}W clusters. The B-B results appear to be less well defined as to strong directions. This may be due in part to the higher sample number.

Inter-consistency

A comparison of the MSS ray diagrams between the two groups only shows a reasonable similarity in the N-S component. The maxima directions of each are not the same.

The radar scenes yielded a closer comparison. Both of the directions in Sanderson's diagram appear as perhaps secondary and tertiary prominence on B-B's ray diagram. The primary direction on the B-B diagram is not found on Sanderson's results.

The flight direction of Seasat radar and its westward scan has highlighted the east slope of N-NE trending topographic feature. This is B-B's most prominent direction whereas in Sanderson's diagram it is

virtually absent. Sanderson was aware of the potential bias the shading could have and mentally filtered this effect and with it, undoubtedly, some real linears.

The peak distributions on the merged plots are at right angles to one another and in each group, the respective maxima are the strongest of the three scenes. Sanderson's secondary maxima correlates with B-B's quaternary maxima.

The radar image yielded the best comparison of the three scenes. The comparison, however, is only moderate.

Comparison to field study

The results of the linear determination was compared to a joint study published by Sanderson on the Huntington area. To compare the results, a table was generated having the four principal joint sets identified in the field compared to the results of the ray diagrams. The numbers in the table refer to the order of prominence of the direction on the ray diagram. A "NO" indicates the particular joint set direction didn't prominently appear on the ray diagram.

	Sanderson			Bonnett-Brumfield		
Joint Set	MSS	Radar	Merged	MSS	Radar	Merged
E-W	3	NO	1	NO	NO	NO
N-S	2	NO	NO	1	NO	1
NW-SE	NO	1	2	3	2	NO
NE-SW	1	NO	NO	2	NO	3

Summary of Frequencies

Prominence	Sanderson	Bonnett-Brumfield
1st	3	2
2nd	2	2
3rd	1	2
NO	6	6

The results show that one group was not significantly better than the other in matching linears with major joint sets (if indeed there is such a correlation). One half of the twelve entries for each group resulted in NO's meaning that the remote sensed data did not reveal the joint pattern very well. The radar scan scenes gave the poorest correlation with the field data.

Conclusions

1) Personal bias, training etc., will affect the linear selection.

2) About the same time was needed to complete linear selection for different persons.

3) Numbers of linears selected was not proportional to time investigated.

4) There may or may not be an interval consistency of results of different image scans from the same area.

5) There was only moderate correlation of results between different persons.

6) There was only moderate correlation of linears with joint patterns.

SANDERSON

RAY DIAGRAM OF LINEARS

HUNTINGTON, WV AREA

LANDSAT-MSS

N = 21

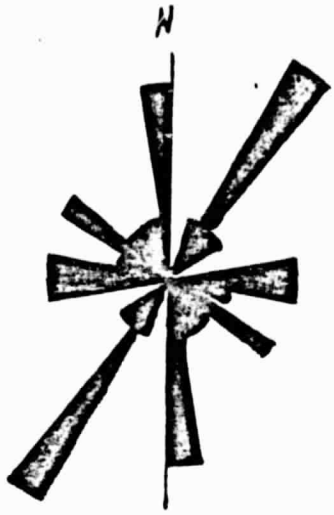

RADAR

N = 37

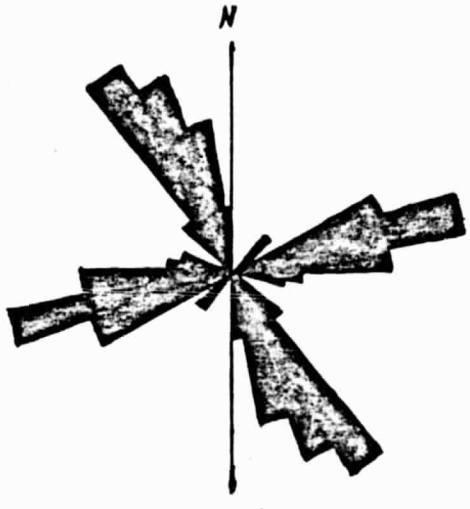

MERGED

N = 35

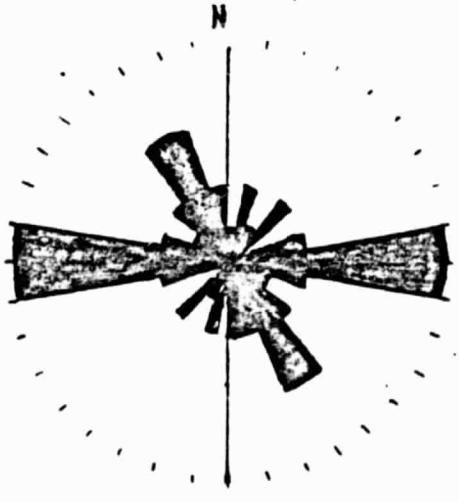

BONNETT-BRUMFIELD

RAY DIAGRAM OF LINEARS

HUNTINGTON, WV AREA

LANDSAT-MSS

N = 78

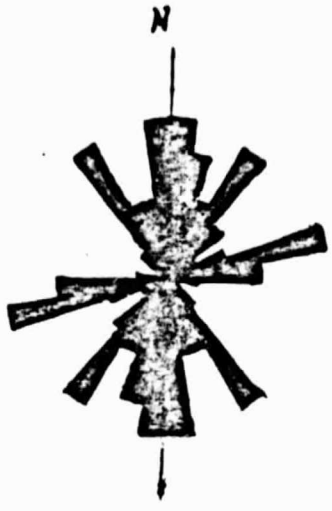

RADAR

N = 94

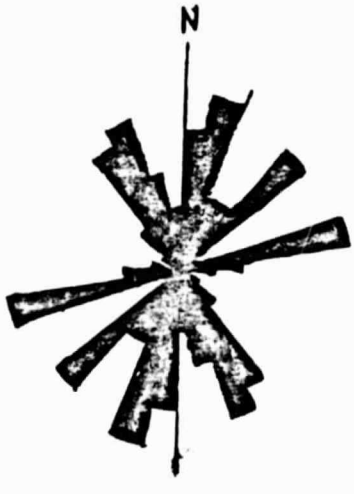

MERGED

N = 125

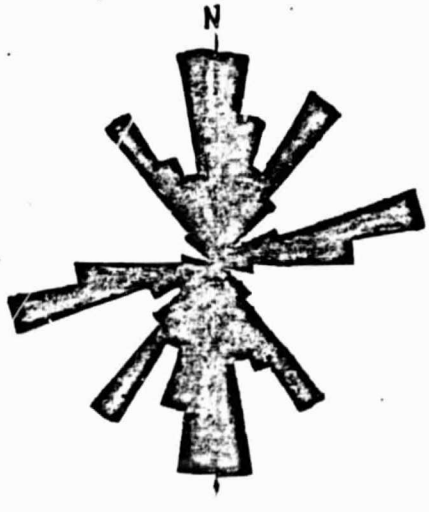

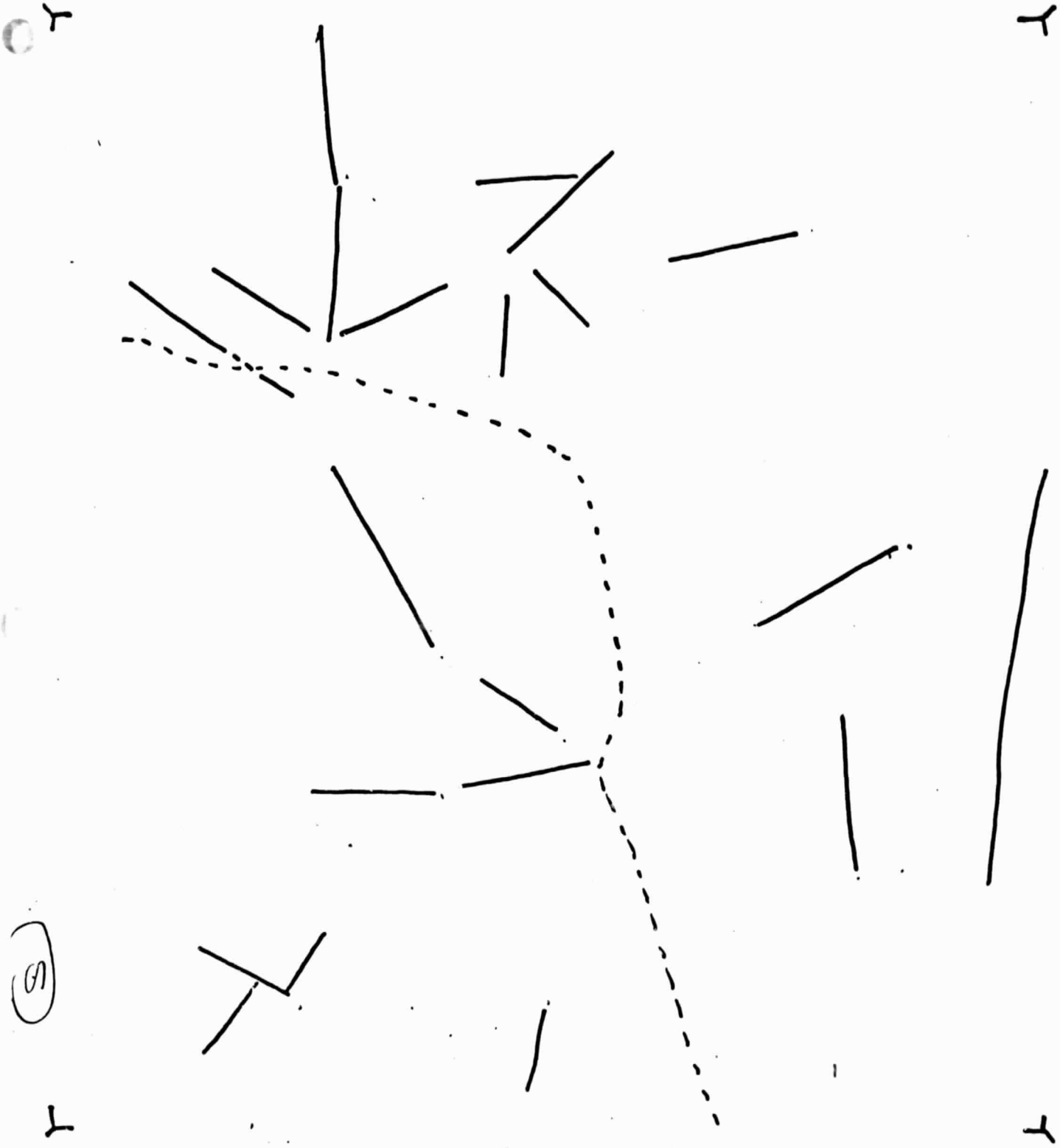

HBS-IDIMS CONTRAST-ENHANCED

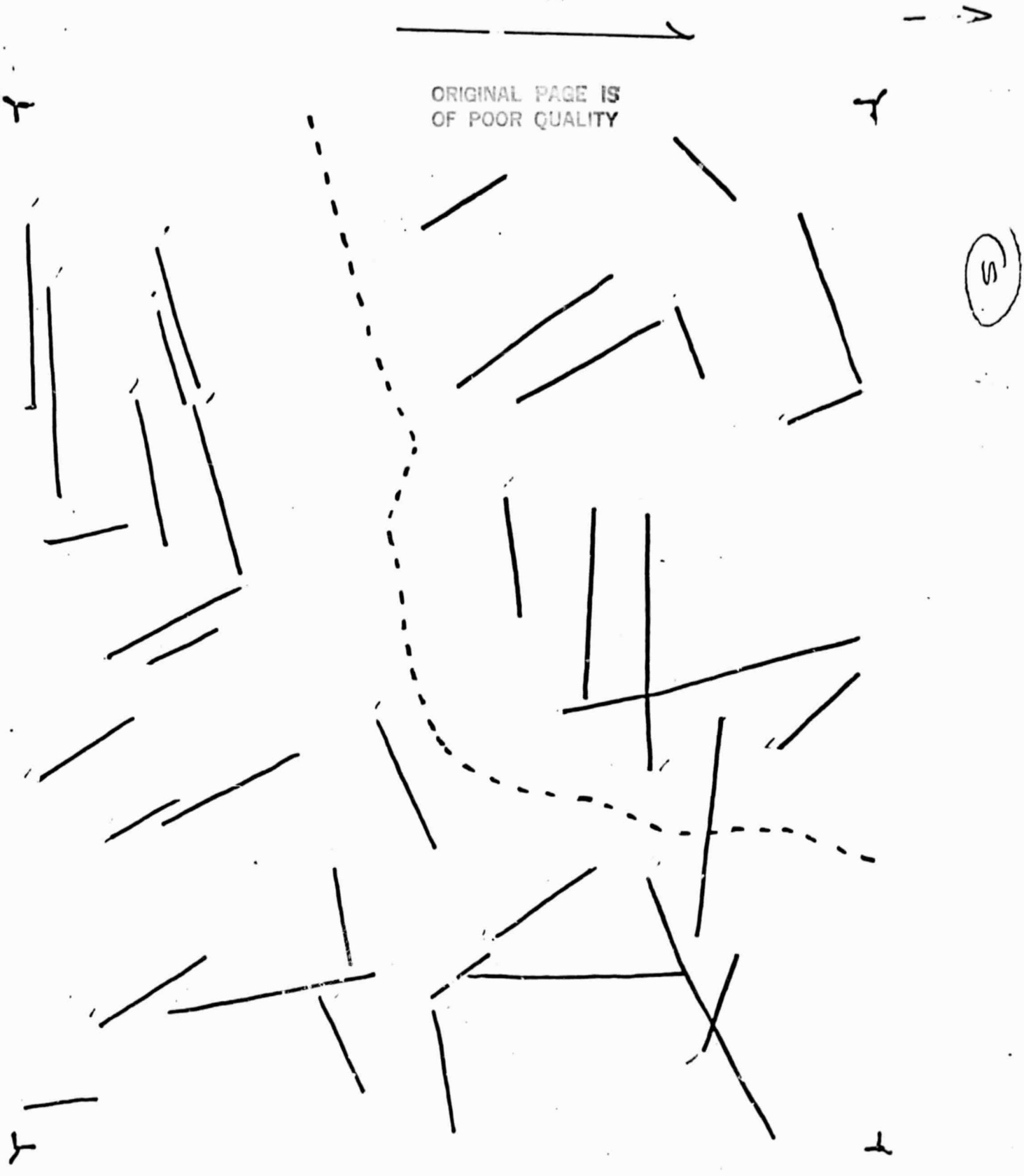

Seasat - SAR Radar - 1978

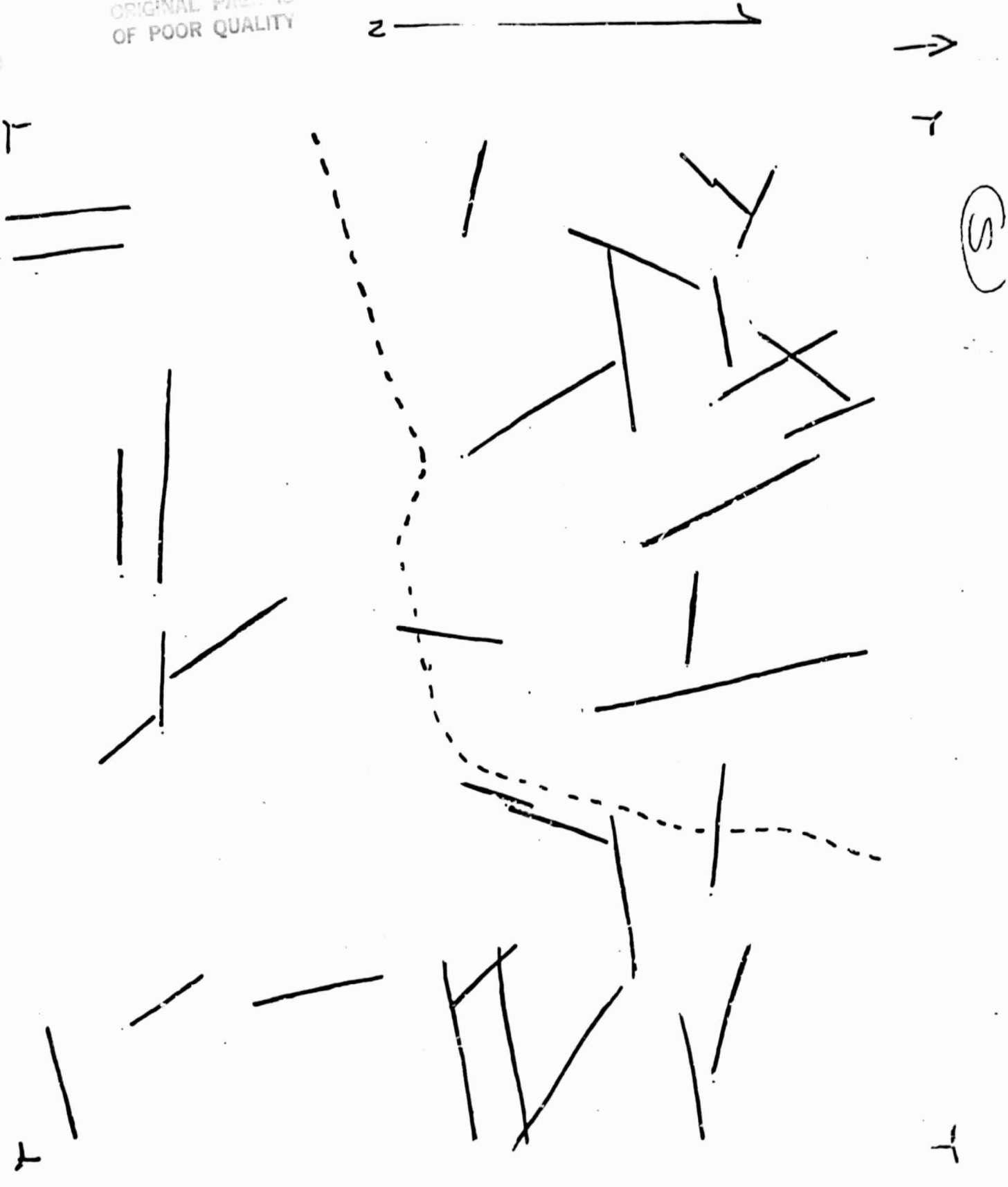

Seasat - HSS Merged

ORIGINAL PAGE IS
OF POOR QUALITY

C-2

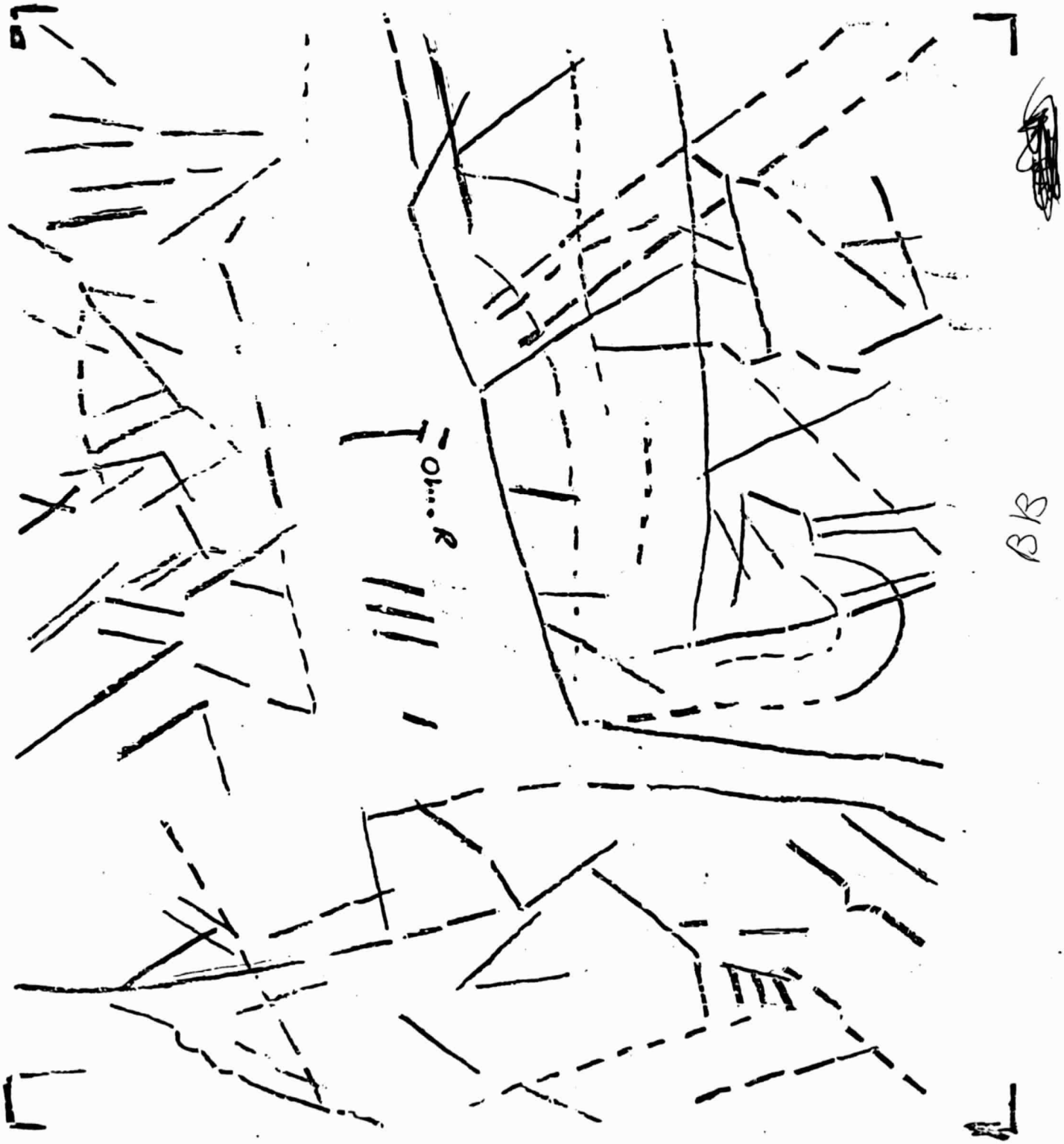

APPENDIX B

TEAM CONSIDERATIONS FOR INTERPRETATION IN LINEAR DETERMINATIONS

Dewey Sanderson, Richard Bonnett & James Brumfield
Remote Sensing Group, Marshall University
Huntington, West Virginia

Orbital altitude imagery using two different sensor systems, LANDSAT and SEASAT were evaluated independently and on merged data sets for linear interpretability in the Huntington, WV region.

An interpretive approach involving two teams independently evaluating the three different imaged data sets provided by Dr. Herb Blodget, NASA/Goddard Space Flight Center was employed. Both teams have training and experience in imagery interpretive techniques and various levels of training and experience with LANDSAT and SEASAT Data sets. The rationale for the selection of linears was not identical in each of the two teams results. The Bonnett and Brumfield team's basic decision for interpretation was to identify those features which suggested linearity whether strongly expressed in drainage patterns or more subtle tonal and textural variations. An earlier study in the region on stream piracy by Bonnett (1) revealed that some streams were probably joint controlled and therefore after a brief discussion the Bonnett-Brumfield team decided that both the subtle tonal and textural variations as well as the stronger possible joint controlled stream patterns would be interpreted. Sanderson, on the other hand independently decided upon a criteria of subtle tonal variations in linear interpretation in his study. Also in interpretation of SEASAT data, each team made an independent decision concerning criteria for interpretation. Bonnett-Brumfield, after considering look directions and other factors influencing the return signal decided to interpret those features which were strongly ex-

pressed as possible joint controlled stream patterns and the more subtle tonal and textural variations. The Bonnett-Brumfield team also recognized that the look direction will probably bias the data for linears. Sanderson, on the other hand, decided to mentally filter these look direction biases for strongly related features and may have inadvertently filtered out subtle tonal expressions in the bias as well.

All in all, the interpretability of the merged data sets were considered by both teams the more easily interpreted. Sanderson felt the SEASAT was equally interpretable. The results as given in Sanderson's, "Summary of Results" basically compare linear numbers and direction with the rosettes published in an earlier work by Sanderson (2). There was not sufficient time to thoroughly check the results by actual superposition and measurement of the overlay with field derived data. Therefore the summary results are still relatively subjective.

Further studies might include length-stroke orientation analysis, geographic location of linears and reproducibility of the linear study.

References:

(1) Bonnett, Richard, "Analysis of Pleistocene & Holocene Drainage Changes Northwest of the Nitro, WV Region", Proceedings of the West Virginia Academy of Science, Vo. 47, No. 3-4 1975 pp 205-211.

(2) Sanderson, Dewey D. & R. Woodrow Duba, "The Joint Pattern of the Tri-State Areas, West Virginia, Ohio, Kentucky", Proceedings of the West Virginia Academy of Science, Vol. 47 No. 2, 1975, pp 106-113.

APPENDIX C

AN EVALUATION OF LANDSAT MSS & MERGED LANDSAT MSS/SEASAT SAR CLASSIFIED DATA SETS FOR LAND COVER/CATEGORY ANALYSIS

James Roueche, KYOVA Interstate Planning Commission &
James Brumfield, Remote Sensing Group, Marshall U., Huntington, WV

Three orbital altitude classified LANDSAT MSS images from the two consecutive years of 1977 and 1978 and LANDSAT MSS/SEASAT SAR merged data sets and the resulting image classified for the 1978 data provided by Dr. Herb Blodget, NASA/GSFC, Greenbelt, Md., were evaluated for land category accuracy by two methods:

(1) Determination of selected spatial representation for land cover categories of the classified images:

(2) Acreage statistics of the classified categories.

The relative accuracies of the LANDSAT MSS classified images were then compared to the merged LANDSAT MSS/SEASAT classified images. The final results were then evaluated as to overall utilization in meeting regional planning needs.

Discussion Of Methods:

Each of the classified images were analyzed utilizing B-W aerial photography of April 1976* at a scale of 1:24000 and B-W aerial photography of April 1980** at a scale of 1:24000 for selected regions of Cabell County to insure several selected areas of each land cover

*Panchromatic prints 7½' Quad flown in April, 1976 & furnished to the KYOVA Interstate Planning Commission by the U. S. Army Corps. of Engineers, Huntington District.

**Panchromatic prints 18" x 18" flown in April, 1980 & furnished by the KYOVA Interstate Planning Commission by U. S. Army Corps. of Engineers, Huntington District, Huntington, WV.

category in terms of spatial representational accuracies. Then each set of land category statistics for each classified images were compared to a 1968 comprehensive land use planning study for the SMSA including Cabell County with projections thru 1990 for acreage accuracy assessment. Finally the relative accuracies of the LANDSAT MSS classified and merged LANDSAT SEASAT SAR classified images were compared for accuracy of land cover category special representation and over-all category acreage estimates.

Results:

The LANDSAT MSS classified images for 1977 and 1978 data sets were analyzed for land cover category spatial representation and compared. The authors found the overall spatial land cover category relative to land use categories generally quite good. The categories for example on commercial, industrial or high density residential depicted the areas quite well in terms of existing land usage when compared to the authors' interpretation of the 1976 and 1980 aerial photography and authors' knowledge of the area. The estimated locational representation for these three land cover use/categories appears approximately 80 to 85 per cent accurate. Low and medium residential categories appear to depict the land usage pattern well. However, road patterns as confused with those categories. Consequently, aerial extent is apparently overstated. The agricultural category seems to be understated and may be confused with low density residential areas. Limited time and lack of statistical data prevented an analysis of the forested category. However, one might assume that if the other

categories are reasonably correct, then the forested category would be relatively correct. The water category depicts the Ohio River whereas the Guyandotte River and several three to eight acre ponds and treatment facilities are not evident. There was no bare ground evaluation made. A portion of the unclassified category, however, appears to be the Guyandotte River and the rest of that category apparently mixed pixel problems. Because of small scale and perhaps no detectable change in the area, no significant difference in categories could be determined between 1977 and 1978 LANDSAT MSS classified images by visual inspection.

The LANDSAT MSS and merged LANDSAT MSS/SEASAT SAR classified images were analyzed for land category spatial representation. The authors found the overall spatial representation of land cover categories relative to general land-use categories quite good. The land cover/use categories for commercial, industrial, high density residential depicted these areas remarkable well in terms of location for existing land-use patterns when compared to the author's interpretation for the 1976 and 1980 years aerial photography and the author's knowledge of the area. The estimated locational accuracy appears to approach ninety percent. Low and medium density residential categories seem to depict the land-usage patterns quite well, however road patterns are confused with these categories. Consequently, aerial extent is apparently overstated. The agircultural category as before appears to be understated and confused with low-density residential. Forrested categories were not evaluated for the previously

stated reasons. The water categories did depict a sewage treatment pond in addition to the Ohio River, however, other ponds and the Guyandotte River were not represented.

Acreage comparisons of selected LANDSAT MSS and merged LANDSAT MSS/SEASAT SAR classified categories were compared with acreage estimates from a comprehensive planning study (1) which includes Cabell County and is compiled in table I.

Land Use Cover/ Categories	Comprehensive Study Acreage	MSS 1977 Acreage	MSS 1978 Acreage	MSS-SAT 1978 Acreage
High Density Res.	Total	3051	2709	2531
Med. Density Res.	Residential	7728	8172	8573
Low Density Res.		18,540	18,015	17,620
TOTAL Residential	6853	29,370	28,896	28,724
Commercial	1079	757	924	1,221
Industrial	1562	532	317	624

LANDSAT MSS & merged LANDSAT MSS/SEASAT SAR classification comparisons.

The low and medium residential classification relative to acreage is extremely optimistic when compared with existing figures from the comprehensive study (1) by approximately 500 per cent. However, the merged LANDSAT MSS/SEASAT SAR classification categories for high and medium residential depict the overall location quite well in terms of land usage patterns whereas the LANDSAT MSS classification in the opinion of the authors tends to over-emphasize medium residential land-usage patterns. Agriculture and low-density residential categories appear to be confused on both the LANDSAT MSS and merged LANDSAT MSS/SEASAT SAR classified images. Also, there is confusion on both classification formats of road patterns with medium and low-density residen-

tial. Additionally smaller rivers and ponds tend to be mis-classified except a waste-treatment pond which was correctly classified on merged classification. Commercial, industrial, and high-density residential areas were all identified with reasonable accuracy in terms of existing land-use patterns. The merged classified image appears to more accurately depict and locate these categories when compared to the authors' interpretation of the aerial photography and the authors' knowledge of the area.

Conclusions:

It would appear on the basis of the authors' analysis and comparisons of the image data sets that the merged LANDSAT MSS/SEASAT SAR classified image would be the most suitable for regional planning activities. However, the confusion of roads with medium and low-density residential and low-density residential with agriculture patterns would suggest their utility for very generalized planning. Resolution of these problems would clearly enhance the utilization for more specific planning. With current trends by various sources in deemphasizing funding for long-range planning activities of this nature, monitoring general land-cover/use categories on an annual or bi-annual basis could aid in analysis of changes for land-use patterns and land development.

Reference:

(1) KYOVA Interstate Planning Commission,
"Schematic Land Use Study", February 1973, pp 10-21.

APPENDIX D

WEST VIRGINIA
GEOLOGICAL AND ECONOMIC SURVEY

Robert B. Erwin, *Director*
and *State Geologist*

P. O. Box 879
Morgantown, WV 26505
304/292-6331

Offices at Mont Chateau
Mont Chateau Road
Exit 10 (Cheat Lake) off U.S. 48

IN REPLY REFER TO:
EV/8640/0083/036/81

February 5, 1981

Mr. Herb W. Blodget
ERRSAC - NASA 902.1
Goddard Space Flight Center
Greenbelt, MD 20771

Dear Herb,

Sorry for the delay with this information, but things just don't go according to Hoyle. I've taken a close look at the land use data derived from Landsat and Seasat for Cabell County and generated the following table.

Acres

	Color IR WVG&ES	*Landsat NASA*	*Landsat & Seasat NASA*
Water	*3,539*	*2,659*	*2,916*
Forest	*146,692*	*133,942*	*136,122*
Agriculture	*16,655*	*13,240*	*11,320*
Barren Land	*277*	*0*	*0*
Urban Total	*15,222*	*30,659*	*30,569*
High density	*10,359*	*10,780*	*11,104*
Res. Med. density			
Low density	*-*	*18,590*	*17,620*
Grand Total	*182,602*	*181,374*	*181,370*

As you can see, there are some differences: the major ones being a lower Forest acreage for Landsat and a higher Urban acreage for Landsat. I examined the color IR photography, topo maps, and our Land Use Map and believe Landsat Low density residential is the source. If Low density residential was changed to Agriculture and Forest, then the acreage would be in better agreement.

Such a modification must be based on your definition of Low density residential and how the computer was trained to generate the picture and statistics.

Now, I have just one question: what is the total cost per square mile to generate a similar land use map from Landsat for the entire State? Assume that it would be done by a commercial outfit at a scale of 1:250,000.

I hope this helps you out.

Best regards,

Peter Lessing
Division Chief

PL:lc

APPENDIX E

EASTERN KENTUCKY UNIVERSITY

Richmond, Kentucky 40475

COLLEGE OF SOCIAL AND BEHAVIORAL SCIENCES
Department of Geography and Planning

206 Roark Building
606-622-2251

February 4, 1981

Dr. Herb W. Blodget
Eastern Regional Remote
Sensing Applications Center
NASA, Goddard Space Flight Center
Greenbelt, Maryland
20771 Attn. 902.1

Dear ~~Dr. Blodget~~ Herb,

In accordance with your request, the MSS image and the merged MSS-Seasat image were evaluated to determine their usefulness in land cover and geological studies. The images were evaluated first by sampling selected identical areas on both images to note changes in classification. A comparison was then made of the land cover shown on the images with that shown on other imagery and maps. To aid in the comparison of the two 1:250,000 scale images grid overlays divided into one-half square inch units were attached in an identical fashion to each image (see enclosure). The images were then placed on a Bausch and Lomb Zoom Transfer Scope model ZT4 so that the MSS-Seasat image was projected at an identical scale onto the MSS image. Illumination was adjusted to full intensity using front and backlighting for the merged MSS-Seasat image. By rapidly manipulating the rheostat switch to alternately increase and decrease light intensity on the MSS image, the areas that were classified differently could readily be identified. Selected areas were examined in various parts of the county. The results of this examination are presented below:

Classification Changes in Land Cover

Coordinates	From (on MSS image)	To (on merged MSS-Seasat image)
H-6	high density res.	low & med. dens. res.
	low dens. res.	agric.
	forest	low & med. dens. res.
H-7	low dens. res.	agric.
	med. dens. res.	low dens.
	forest	low dens.
H-8	low dens. res.	forest
	low dens. res.	med. dens. res. 1
	med. dens. res.	low dens. res.
H-9	low dens. res.	agric.
	low & med. dens. res.	forest

H-10	low dens. res.	agric.
	med. dens. res.	low dens. res.
	med. dens. res.	industry
H-11	med. dens. res.	low dens. res.
	agric.	low dens. res.
J-11	agric.	low dens. res.
J-10	agric.	low dens. res.
J-9	agric.	low dens. res.
	med. dens. res.	low dens. res.
J-8	low dens. res.	agric.
J-7	low dens. res.	agric.
	low dens. res.	forest
H-13	low dens. res.	forest
	low dens. res.	agric.
	med. dens. res.	low
H-14	med. & high dens. res.	industry
	med. dens. res.	low dens. res.
	high dens. res.	med. dens. res.
H-15	industry	high dens. res.
	high dens. res.	med. dens. res. 1
	industry	med. dens. res.
	high & med. dens. res.	industry
H-16	industry	high dens. res.
	high dens.	med. dens. res.
H-17	high dens. res.	med. dens. res.
G-3	med. dens. res.	low dens. res.
	low dens. res.	agric. & forest
G-4	low dens. res.	agric. & forest
	med. dens. res.	low dens. res.
G-5	low dens. res.	agric. & forest
	med. dens. res.	low dens. res.
F-5	low dens. res.	agric. & forest
F-6	low dens. res.	agric. & forest

The classification of the merged MSS-Seasat images generally caused a shift from a higher order of land use/cover to a lower order of land use/cover. Seventy four percent of the classification changes in the areas examined were of this type. The most frequently occurring change was the

reclassification of low density residential to agricultural land uses. This was closely followed by the reclassification of low density residential to forest, and by medium density residential to low density residential. Portions of images covering urban areas often showed more commercial and industrial areas on the merged image.

The merged MSS-Seasat data appear to present a more accurate distribution of land cover. This must be accepted as a tentative conclusion. A comparison was made between the distribution of land cover as shown on the two images and what could be inferred or determined from 1:250,000 scale topograph maps and the enhanced imagery used in the Appalachian Lineament Analysis Project. From this comparison the distribution and the categorization of land cover from the merged data appear to be more correct than that shown on the image derived from Landsat data. A more accurate evaluation could have been made if recent aerial photography of the county had been available.

The two images have limited usefulness for geological applications. Structure and lineament information may be more easily noted on standard Landsat or Seasat images. The special enhancements produced for the Appalachian Lineament Analysis are also much superior for geological applications. It is possible that the algorithms used to produce the land cover classifications may have some application to geological studies in arid portions of the world where signatures for rock types may be more easily established. In these regions merged data from Landsat and Seasat may be as useful in discriminating between rock types as it apparently is in discriminating between categories of land cover.

Sincerely yours,

Bill Adams

William G. Adams
Associate Professor

WGA/mkk

Enclosure

AREAS EVALUATED

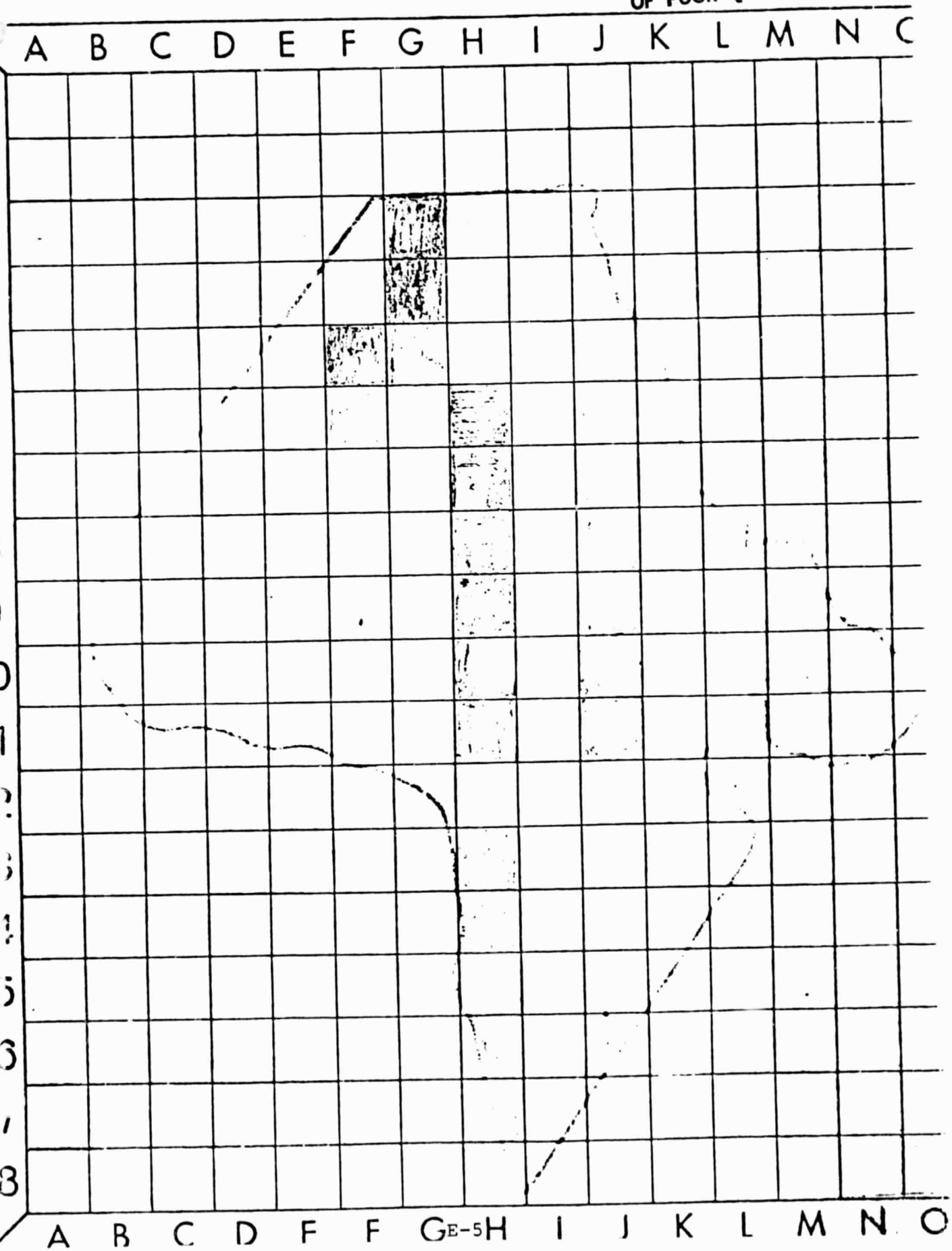

REFERENCES

1. R. Barthelemy and A. Dempster, "Geological Interpretation of the ERTS-1 Satellite Imagery of Lesotho, and Possible Relations Between Lineaments and Kimberlite Pipe Emplacement," Proceedings Tenth International Symposium on Remote Sensing of Environment, Environmental Research Institute of Michigan, Ann Arbor, 1975, pp. 915-924

2. H. Blodget (Editor), "Appalachian Lineaments Analysis ASVT Workshop," Eastern Regional Remote Sensing Applications Center, Goddard Space Flight Center, Greenbelt, Maryland, 1980, 41 p.

3. M. L. Bryan, "Analysis of Two Seasat SAR Images of an Urban Scene," 47th Annual Meeting, The American Society of Photogrammetry, Washington, D.C., February 22-27, 1981

4. W. J. Campbell, "ERRSAC Interactive Computer System for Image Processing," Internal Document, Eastern Regional Remote Sensing Application Center, Goddard Space Flight Center, Greenbelt, Maryland

5. W. D. Carter and L. C. Rowan, "A World Wide Approach to Remote Sensing and Mineral Exploration," Proceedings 12th International Symposium on Remote Sensing of Environment, Environmental Research Institute of Michigan, Ann Arbor, 1978, pp. 387-394

6. G. J. Chafaris, "Definition of the Major Applications and Requirements Relative to Overlaying Seasat-1 SAR and Landsat MSS Data Sets," General Electric, Beltsville, Maryland, Final Report June 8, 1978

7. J. Clark, "Improved Land Use Classification From Landsat and Seasat Satellite Imagery Registered to a Common Map Base," 47th Annual Meeting, The American Society of Photogrammetry, Washington, D.C., February 22-27, 1981

8. S. Cox, and N. Roller, "Comparison of Landsat MSS and Merged MSS/RBV Data for Analysis of Natural Vegetation," Proceedings of the Fourteenth International Symposium on Remote Sensing of Environment, San Jose, Costa Rica, 1980

9. ESL Inc., "IDIMS User's Guide," Technical Memorandum ESL-TM705, Supplement 1, Electromagnetic Spectrum Laboratory, Sunnyvale, California, February 1977

10. J. P. Ford, "Seasat Orbital Radar Imagery for Geologic Mapping: Tennessee-Kentucky-Virginia," American Association of Petroleum Geologists Bulletin, vol. 64, no. 12, pp. 2064-2094, December 1980

11. Goddard Space Flight Center, "ERTS Data User's Handbook," Document No. 71 SD 4249, Section 2: Revised February 15, 1972

12. A. F. H. Goetz, F. Billingsley, D. P. Elston, I. Lucchitta, and E. M. Shoemaker, "Geologic Applications of ERTS Images on the Colorado Plateau, Arizona," Third Earth Resources Technology Satellite-1 Symposium, National Aeronautics and Space Administration Special Publication 351, Washington, D.C., 1974, pp. 719-744

13. A. Goetz, and L. C. Rowan, "Geologic Remote Sensing," Science, Vol. 211, February 20, 1981

14. F. J. Gunther, "A New Procedure for Principal Components Analysis of Landsat MSS Images for Rock Differentiation," Computer Sciences Corporation, CSC/TM-80/6160, June 1980

15. W. R. Hemphill, and W. Danilchik, "Geologic Interpretation of a Gemini Photo," Photogrammetric Engineering, Vol. 34, No. 2, February 1968, pp. 150-154

16. A. V. Heyl, "The 38th Parallel Lineament and its Relation to Ore Deposits," Econ. Geol., Vol. 67, 1972, pp. 879-894

17. W. H. Hobbs, "Earth Features and Their Meaning: An Introduction to Geology for the Student and General Reader," Macmillan Co., New York, 1912

18. Hoffer, M. and Staff, "Techniques for Computer-Aided Analysis of ERTS1-1 Data, Useful in Geologic, Forest and Water Resource Surveys," Third Earth Resources Technology Satellite-1 Symposium, National Aeronautics and Space Administration Special Publication 351, Washington, D.C., 1974, pp. 1687-1708

19. R. S. Houston, R. W. Marrs, R. M. Brockenridge, and D. L. Blackstone, Jr., "Application of the ERTS System to the Study of Wyoming Resources with Emphasis on the Use of Basic Data Products," Third Earth Resources Technology Satellite-1 Symposium, National Aeronautics and Space Administration Special Publication 351, Washington, D.C., 1974, pp. 595-619

20. Y. W. Isachsen, "Spectral Geological Content of ERTS1-1 Imagery Over a Variety of Geological Terrain in New York State," Symposium Proceedings, Management and Utilization of Remote Sensing Data, The American Society of Photogrammetry, Falls Church, Virginia, 1973, pp. 342-363

21. Y. W. Isachsen, R. H. Fakundiny, and S. W. Forste, "Evaluation of ERTS Imagery for Spectral Geological Mapping in Diverse Terrain of New York State," Third Earth Resources Technology Satellite-1 Symposium, National Aeronautics and Space Administration Special Publication 351, Washington, D.C., 1974, pp. 691-717

22. P. L. Jackson, H. L. Wagner, and R. A. Shuchman, "Final Report, Geologic Remote Sensing Over the Cottageville, West Virginia, Gas Field," Environmental Research Institute of Michigan, Ann Arbor, Feburary 1979, 96 p.

23. G. O. Johnson, "Correlation of Landsat Lineaments with Devonian Gas Fields in Lawrence County, Ohio," Eastern Regional Remote Sensing Applications Conference, National Aeronautics and Space Administration Conference Publication 2173, Washington, D.C., January 1981, pp. 69-73

24. Kentucky-Ohio-West Virginia Interstate Planning Commission, "Schematic Land Use Study," February 1973, pp. 10-21

25. P. Lessing, "West Virginia Lineament Study Final Report for Appalachian Regional Commission," West Virginia Geological and Economic Survey, Huntington, West Virginia, 1978

26. P. D. Lowman, Jr., "Geologic Uses of Earth-Orbital Photography," Publication X-644-71-359 Goddard Space Flight Center, Greenbelt, Maryland, 34 p., 1971

27. P. D. Lowman, Jr., J. A. McDivitt, and E. H. White II, "Terrain Photography on the GEMINI IV Mission: Preliminary Report," NASA Technical Note D-3982, National Aeronautics and Space Administration, Washington, D.C., June 1967, 15 p.

28. H. E. Maurer, J. D. Oberholtzer and P. E. Anuta, "Synthetic Aperture Radar/Landsat MSS Image Registration," NASA Reference Publication 1039, June 1979

29. H. Maurer and P. Clemens, "Assembly and Analysis of SAR/Landsat Data Sets," Proceeding of the Purdue/LARS Symposium on Machine Processings of Remotely Sensed Data, June 1977

30. J. G. Moik, "User's Guide for Batch Operation of the SMIPS-VICAR Image Processing System." Publication X-933-76-114, Goddard Space Flight Center, Greenbelt, Maryland, May 1976

31. S. M. Nicolais, "Mineral Exploration with ERTS Imagery," Third Earth Resources Technology Satellite-1 Sumposium, National Aeronautics and Space Administration Special Publication 351, Washington, D.C., 1974, pp. 785-786

32. C. Onasch, "Appalachian Lineament Analysis - Task Report," (NASA Task #20700), Computer Sciences Corporation, Silver Spring, Maryland, 1979

33. M. H. Podwysocki, "FORTRAN IV Programs for Summarization and Analysis of Fracture Trace and Lineament Patterns," Publication X-644-74-3, Goddard Space Flight Center, Greenbelt, Maryland, 44 p., 1974

34. M. H. Podwysocki, "An Analysis of Fracture Trace Patterns in Areas of Flat-lying Sedimentary Rocks for the Detection of Buried Geologic Structure," Publication X-923-74-210, Goddard Space Flight Center, Greenbelt, Maryland, June 1974, 67 p.

35. M. H. Podwysocki, and D. P. Gold, "The Surface Geometry of Inherited Joint and Fracture Trace Patterns Resulting from Active and Passive Deformation," Publication X-923-74-22, Goddard Space Flight Center, Greenbelt, Maryland, July 1974, 38 p.

36. M. H. Podwysocki, J. G. Moik, and W. C. Shoup, "Qualification of Geologic Lineaments by Manual and Machine Processing Techniques," Publication X-923-75-183, Goddard Space Flight Center, Greenbelt, Maryland, July 1975, 23 p.--and--Proceedings of the NASA Earth Resources Survey Sumposium, Lyndon B. Johnson Space Center, Houston, Texax, 1976, pp. 885-903

37. H. K. Ramapriyan, F. J. Gunther, D. P. Helfer, R. L. McKinney and K. P. Young, "Intralab Interi Report II," Computer Sciences Corporation, CSC/TR-77/6004, 1977

38. F. F. Sabins, Jr., "Remote Sensing-Principles and Interpretations," W. H. Freeman and Co., San Francisco, CA., 1978.

39. D. Sanderson and R. Duba, "The Joint Pattern of the Tri-State Areas, West Virginia, Ohio, Kentucky," Proceeding of the West Virginia, Academy of Science, Vol. 47, No. 2, pp. 106-113, 1975

40. N. Short, "Exploration for Fossil and Nuclear Fuels From Orbital Altitudes," Publication X-923-74-322, Goddard Space Flight Center, Greenbelt, Maryland, 53 p., 1974

41. N. Short, P. D. Lowman, Jr., S. C. Freden, and W. A. Finch, Jr., "Mission to Earth: Landsat Views the World," NASA Document SP-360, 1976, NASA Washington, D.C.

42. N. Short, R. Stewart, J. Bensko, M. Blanchard, A. Geotz, M. Podwysocki, M. Abrams, A. Kahle, and B. Siegal, "Practical Applications for Landsat Data for Earth Resources Surveys: Mineral/Energy Resources," NASA Internal Document, Lyndon B. Johnson Space Center, Houston, Texas

43. R. Shuchman, P. Jackson, F. Ruskey and H. Wagner, "Geological Reconnaissance of an Oil Shale Region by Remote Sensing Techniques," Remote Sensing of Earth Resources, vol. V, 1976

44. A. F. Smith and J. E. Miller, "Evaluation of Computer-Enhanced Landsat Imagery for Lineament Analysis and Other Geological Applications," Phase One Report, General Electric, Beltsville, Maryland, 1980

45. S. Stauss, B. Wicinas and J. Ryan, "Data Stratification and the Geographic Entry System (GES): A User's Manual," Technical Memorandum ESL-TM991, Electromagnetic Spectrum Laboratory, Sunnyvale, California, August 1978

46. G. J. Vanderbrug, and A. Rosenfeld, "Linear Feature Mapping," IEEE Transactions on Systems, Man, and Cybernetics, vol. SMC_8, no. 10, October 1978, pp. 768-774

47. M. T. Whalberg, "DICOPAK User's Guide," Publication CSC/TM-77/6080, Computer Sciences Corporation, Silver Spring, Maryland, March 1977

48. E. Werner, "Photolineament Mapping in the Appalachian Plateau and Continental Interior Geological Provinces--A Case Study," Remote Sensing of Earth Resources, vol. V, 1976

49. T. F. Wescott and A. F. Smith, "Product Service and Evaluation of Computer Enhanced Landsat Imagery,' Processing Technique Report, General Electric Beltsville, Maryland, 1979

50. West Virginia Geological and Economic Survey, "Landsat Linear Features of West Virginia, West Sheet," Publication Number WV-7A, 1979

51. West Virginia Geological and Economic Survey, "Land Use Statistics for West Virginia, Part 2," Environmental Geology Bulletin No. 18-1, 1980

52. C. E. Wier, F. J. Wobber, O. R. Russell, R. V. Amato, and T. V. Leshendok, "Relationships of Roof Falls in Underground Coal Mines to Fractures Mapped on ERTS-1 Imagery," Third Earth Resources Technology Satellite-1 Symposium, National Aeronautics and Space Administration Special Publication 351, Washington, D.C., 1974

53. J. T. Wilson, "Structural Features in the Northwest Territories," Amer. Jour. Sci., vol. 239, pp. 493-502, 1941

54. S. T. Wu, "An Improvement in Landcover Classification Achieved by Merging Microwave Data with Landsat Multispectral Scanner Data," ACSM-ASP Convention, St. Louis, Missouri, March 9-14, 1980

55. C. Wu, B. Barkan, B. Huneycutt, C. Leang, and S. Pang, "An Introduction to the Interim Digital SAR Processor and the Characteristics of the Associated Seasat SAR Imagery," JPL Publication 81-26, Jet Propulsion Laboratory, Pasadena, CA., April 1981

56. W. E. Zirk and S. J. Laboda, "A Relationship between Productivity of Gas Wells and their Locations with report to Lineaments: A Statistical Analysis," Publication METC-CR-78/14, Morgantown Energy Technology Center, Morgantown, West Virginia, 1978